

## AUTUMN COLLEGE ON PLASMA PHYSICS

13 October - 7 November 2003

# MHD Turbulence in the Heliospheric Plasma: Coherent Structures and Large Scale Correlations

**P. Veltri**

**Universita' della Calabria, Dip. di Fisica  
Arcavacata di Rende, Italy**

These are preliminary lecture notes, intended only for distribution to participants.



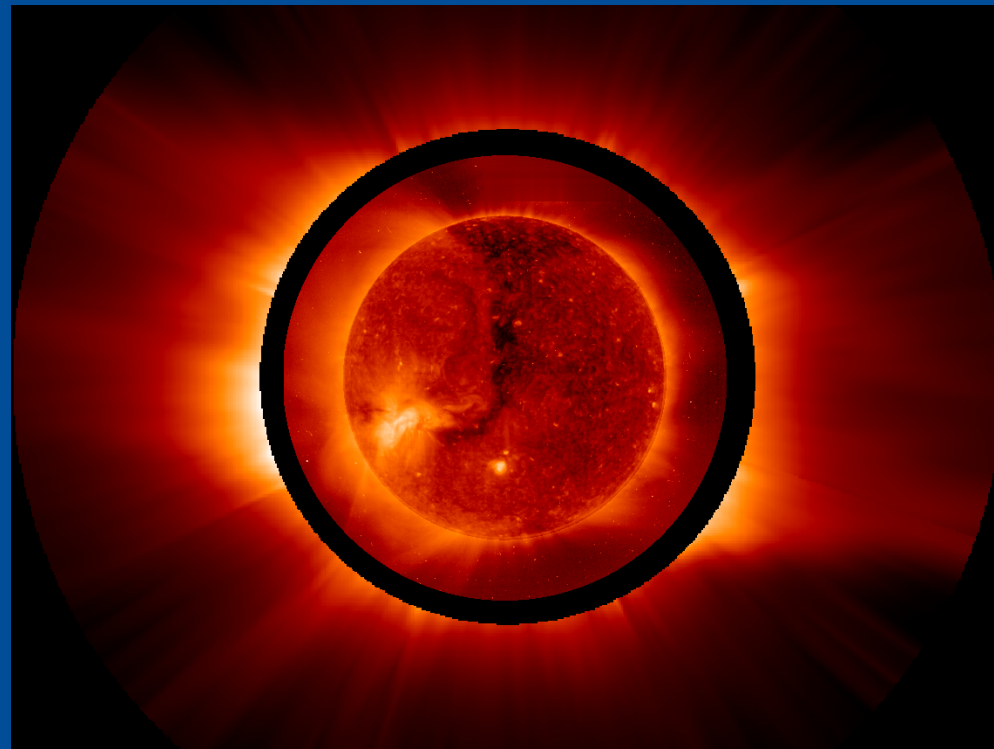
# MHD Turbulence in Heliospheric Plasma: Coherent structures and large scale correlations



Pierluigi Veltri

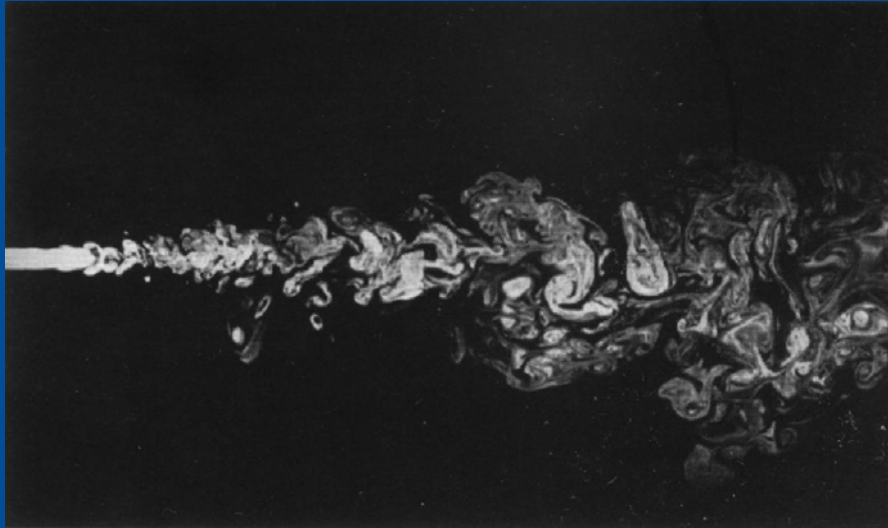
Dipartimento di Fisica, Università della Calabria  
Cosenza - Italy

Pierluigi Veltri  
Dipartimento di Fisica, Università della Calabria



Trieste  
2003

# Main features of turbulent flows



- 1) Randomness both in space and time.
- 2) Turbulent "structures" on all scales within the sea of a random background.
- 3) General unpredictability and instability to very small perturbations.

Turbulence is the result of nonlinear dynamics in DETERMINISTIC (but chaotic) systems

While the details of turbulent motions are extremely sensitive to triggering disturbances, statistical properties are robust quantities

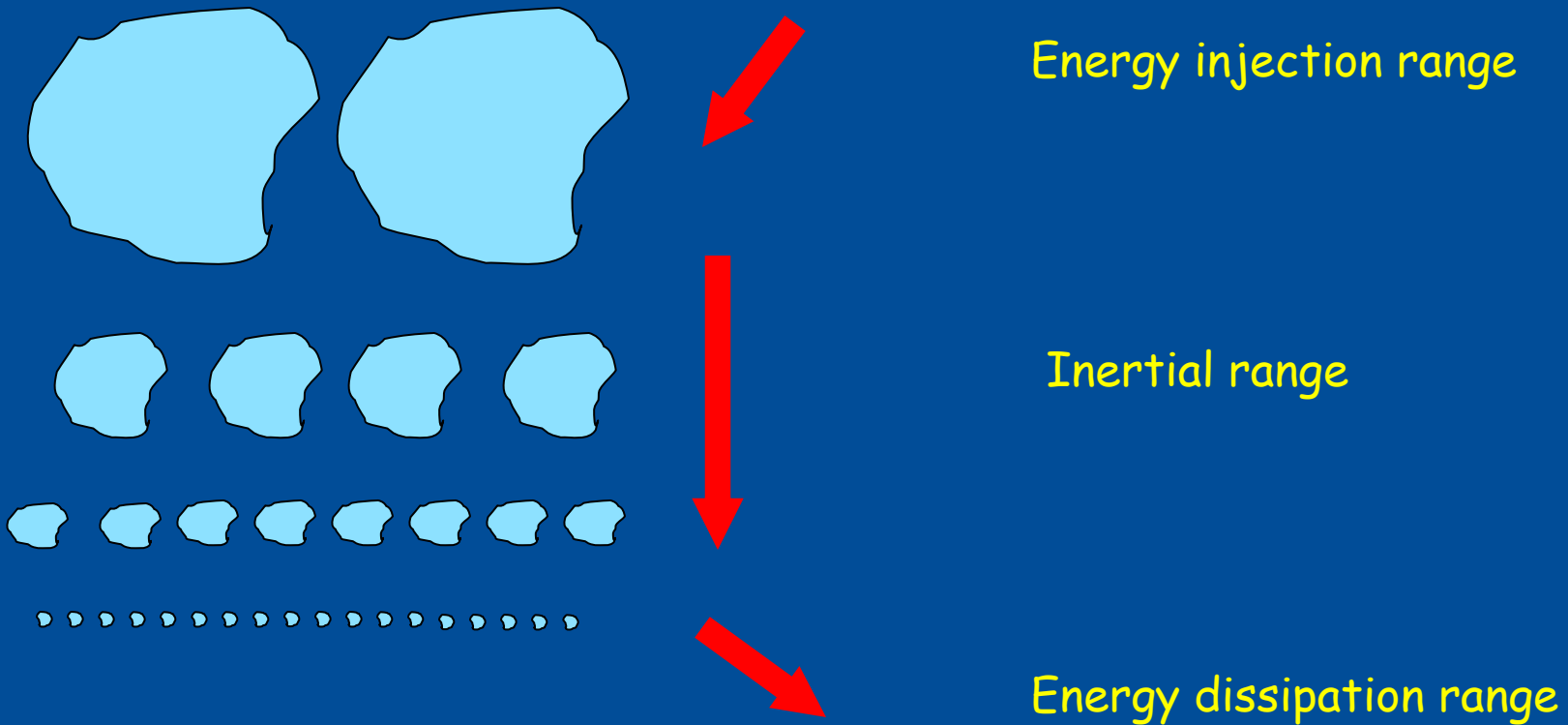
Predictability is reintroduced at a statistical level (via the ergodic theorem and the properties of chaos!).

# The Richardson's picture



Richardson's phenomenology: break down of eddies at large scales and transfer of energy.

Pierluigi Veltri  
Dipartimento di Fisica, Università della Calabria



Trieste  
2003

# Leonardo's view on fluid turbulence



Pierluigi Veltini  
Dipartimento di Fisica, Università della Calabria



Leonardo da Vinci (around 1500 ):

“dove la turbolenza dell'acqua si genera,  
dove la turbolenza dell'acqua si  
mantiene più a lungo,  
dove la turbolenza dell'acqua si posa”

“where the turbulence of water is  
generated,  
where the turbulence of water  
maintains for long,  
where the turbulence of water comes  
to rest”

(Piumati 1894, fo. 74,v - as reported in  
“Turbulence” by U. Frish)

Trieste  
2003

# Modern views on fluid turbulence



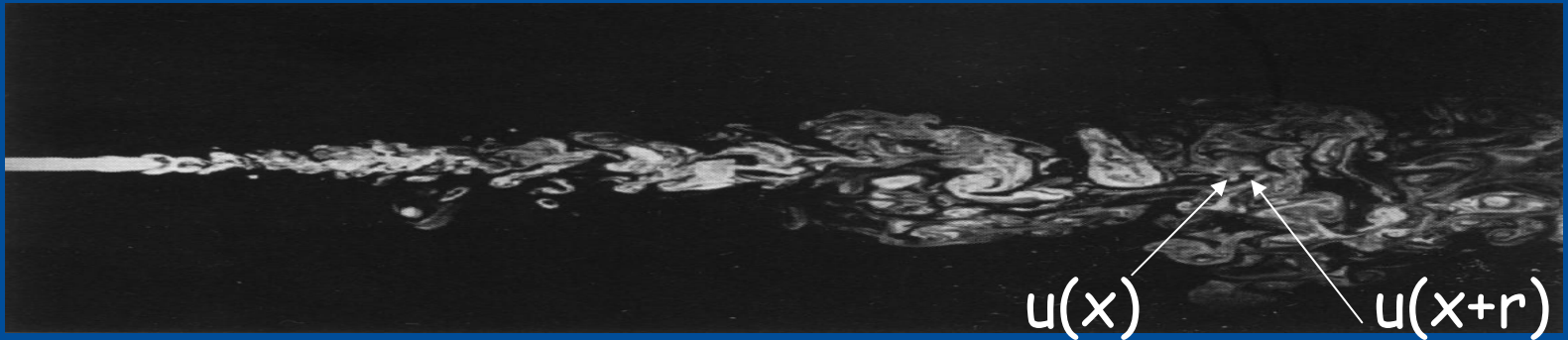
**Sir Horace Lamb (1932):**

"When I die and I go to Heaven, there are two matters on which I hope for enlightenment. One is Quantum Electro-dynamics, and the other is the turbulent motion of fluids. And about the former I am really optimistic"

**K. L. Sreenivasan (Nature, 344, 192; 1990):**

"One no longer needs to go to Heaven to seek enlightenment about Q. E. but, on the Earth turbulence still defies satisfactory description"

# Two-points correlations



Main analysis tools: two-points differences

$$\delta u_r(x) = u(x+r) - u(x)$$

Fluctuations associated to eddies at the scale  $r$ .

Statistical homogeneity 

the 2-th order moment of two-points differences is related to the energy spectrum

$$\langle [\delta u_r(x)]^2 \rangle = 2 \int_0^\infty E(k) \left[ 1 - \frac{\sin kr}{kr} \right] dk$$



# Statistical predictability: universal energy spectrum

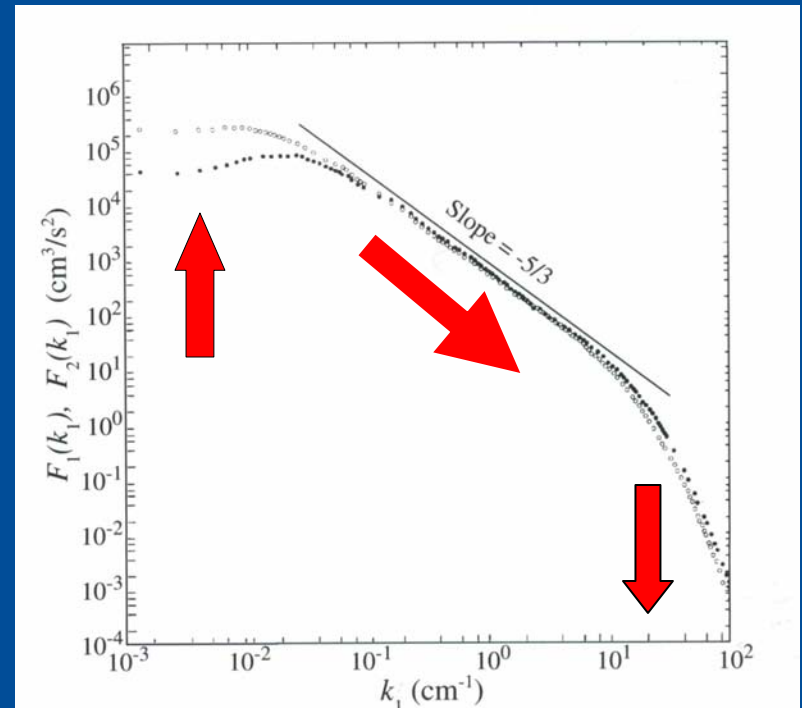


Pierluigi Veltri  
Dipartimento di Fisica, Università della Calabria

Energy input  
at large scale  $L$

Energy cascade  
in the inertial range  
due to non linear  
terms

Energy dissipation  
at small scale  $l_d$



A.N. Kolmogorov:  
in the inertial range  
universal feature

$$\langle \delta u_r^2 \rangle^{1/2} \approx r^{1/3}$$



$$E(k) \approx k^{-5/3}$$

Trieste  
2003

# Solar wind data



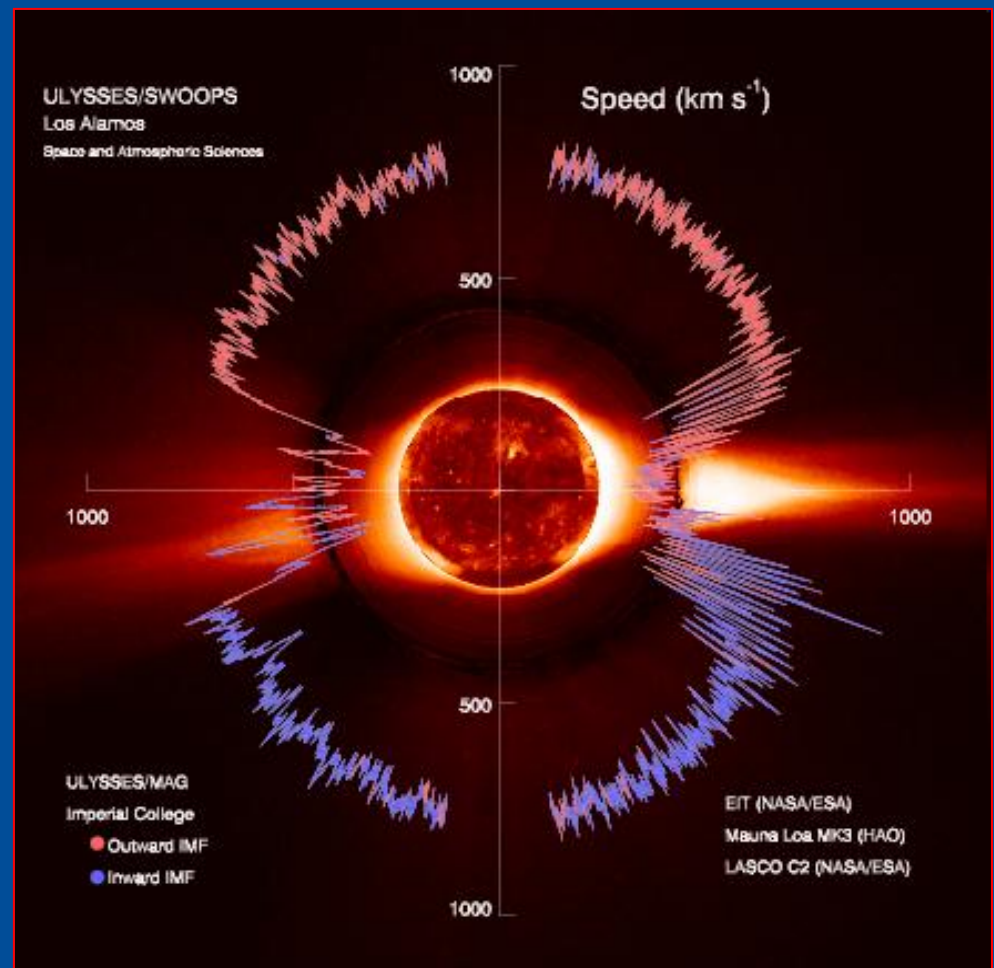
Pierluigi Veltri  
Dipartimento di Fisica, Università della Calabria

Solar wind: a wind tunnel  
Supersonic and  
superalfvenic flow

$$250 \text{ km/s} < V_{\text{SW}} < 800 \text{ km/s}$$

In situ measurements of  
high amplitude fluctuations  
of velocity and magnetic  
fields over 6 decades of  
frequencies (up to ion  
cyclotron frequency)

$$10^{-6} \text{ Hz} < f < 1 \text{ Hz}$$



Trieste  
2003

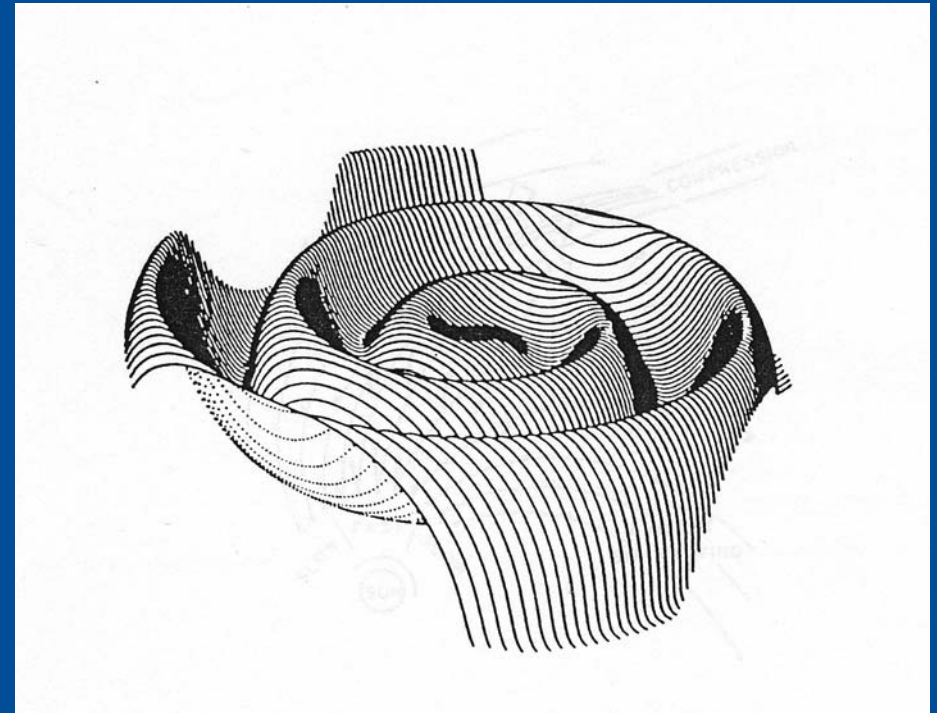
# Heliospheric current sheet



Pierluigi Veltri  
Dipartimento di Fisica, Università della Calabria

A **current sheet** is embedded in the slow wind

In the equatorial region (most widely studied by space experiments):  
Bending of the current structure



**Stream structure**

Fast streams:

$$\begin{aligned}v &\sim 600 - 800 \text{ Km/s} \\n &\sim 1 - 4 \text{ cm}^{-3} \\T &\sim 10^4 - 10^5 \text{ } ^\circ\text{K}\end{aligned}$$

Slow streams:

$$\begin{aligned}v &\sim 250 - 400 \text{ Km/s} \\n &\sim 10 - 40 \text{ cm}^{-3} \\T &\sim 10^3 - 10^4 \text{ } ^\circ\text{K}\end{aligned}$$

Trieste  
2003

# Power law spectrum



Magnetic and velocity fluctuations display a **power law** spectrum extending over more than 5 decades

( $10^{-6} \text{ Hz} < f < 1 \text{ Hz}$ ):

$$W \sim f^{-\alpha}$$

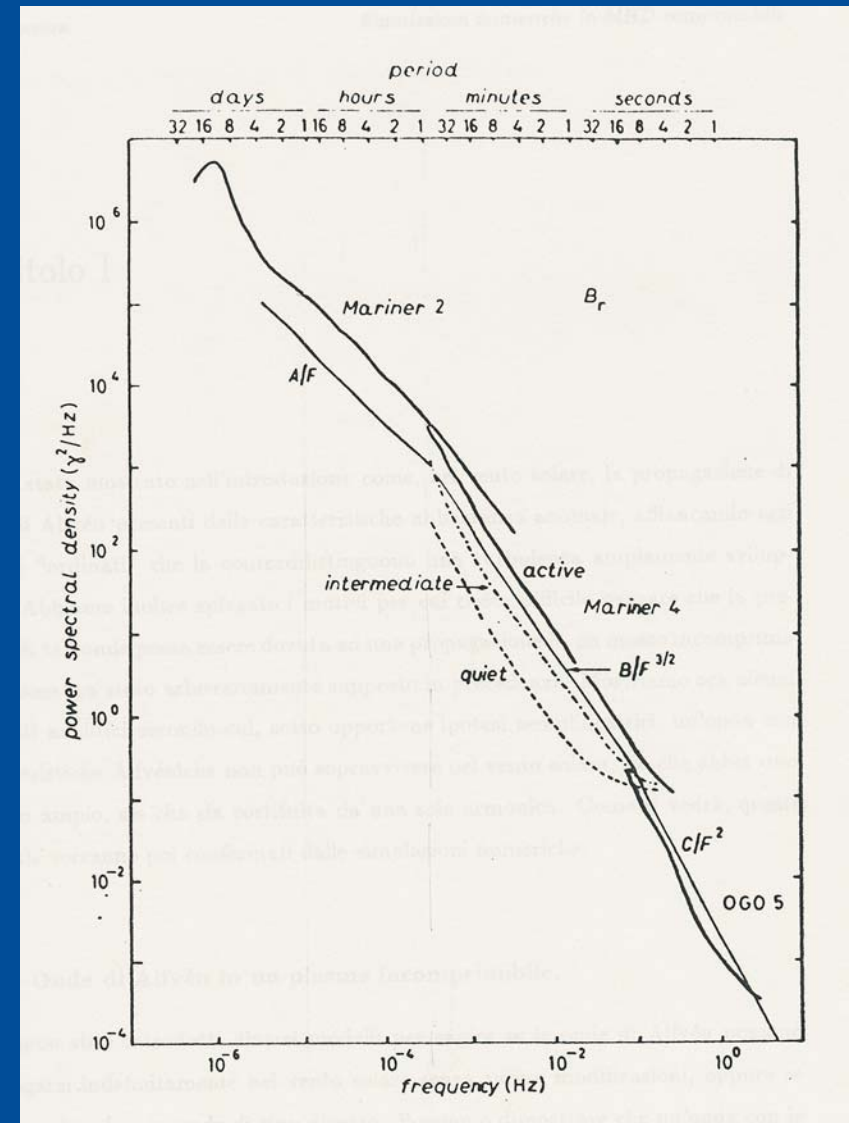
Signature of NL turbulent **energy cascade**

From Taylor hypothesis:

$$L \sim V_{sw} / f$$

Scale range:

$$400 \text{ Km} < L < 1 \text{ AU}$$



# Alfvenic Correlation



In **fast streams**:  
velocity and magnetic  
field fluctuations  
highly correlated

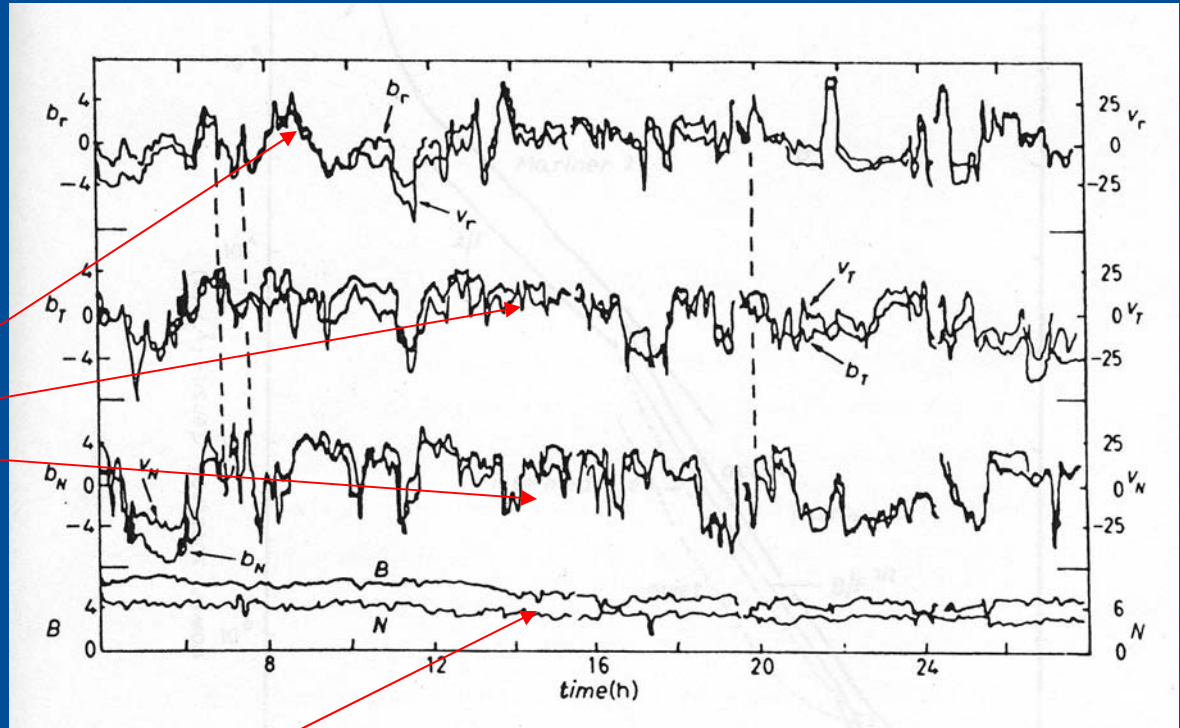
$$\delta \mathbf{v} \sim \sigma \delta \mathbf{B} / (4\pi\rho)^{1/2}$$

$\sigma = +, -$

The sign corresponds  
to

**NL Alfvén waves**  
( $\delta B / B_0 \sim 1$ )

propagating away  
from the sun.



Low level of density and magnetic field intensity  
fluctuations  $\delta\rho/\rho \sim \delta|B|/B_0 \sim$  few percents  
NL effects reduced

In **slow streams**: (i) almost no  $\delta \mathbf{v} - \delta \mathbf{B}$  correlation

(ii) high level of compressive fluctuations

$$\delta\rho/\rho \sim \delta|B|/B_0 \sim 1$$

# MHD equations



Elsasser's variables:

$$\mathbf{z}^\sigma = \mathbf{v} + \sigma \frac{\mathbf{B}}{4\pi\rho}$$

for  
 $\sigma = +1, -1$

MHD equations:

$$\frac{\partial \mathbf{z}^\sigma}{\partial t} + (\mathbf{z}^{-\sigma} \cdot \nabla) \mathbf{z}^\sigma = -\nabla \left( P + \frac{B^2}{8\pi} \right) + \nu \nabla^2 \mathbf{z}^\sigma$$

Nonlinear term

Dissipative term

$$R = \frac{\text{nonlinear}}{\text{dissipative}} \approx \frac{zL}{\nu}$$

The Reynolds number is  
the only parameter of the flow

MHD equations display the same "structure"  
as Navier-Stokes equations

# Alfvenic fluctuations



In a statistically homogeneous medium:

$$\langle \mathbf{B} \rangle = \mathbf{B}_0$$

$$\langle \mathbf{v} \rangle = 0$$

$$\delta \mathbf{z}^\sigma = \delta \mathbf{v} + \sigma \frac{\delta \mathbf{B}}{4 \pi \rho}$$

Elsasser's variables fluctuations

for  $\sigma = +1, -1$

Ideal MHD NL solutions:

$$P + \frac{B^2}{8\pi} = \text{const.}$$

and either

$$\begin{aligned} \delta \mathbf{z}^+ &= 0 \\ \delta \mathbf{z}^- &= \mathbf{F}(\mathbf{r} - \mathbf{v}_A t) \end{aligned}$$



$$\delta \mathbf{v} = -\frac{\delta \mathbf{B}}{4 \pi \rho}$$

or

$$\begin{aligned} \delta \mathbf{z}^+ &= \mathbf{F}(\mathbf{r} + \mathbf{v}_A t) \\ \delta \mathbf{z}^- &= 0 \end{aligned}$$



$$\delta \mathbf{v} = \frac{\delta \mathbf{B}}{4 \pi \rho}$$

# Ideal MHD quadratic invariants



Energy per mass unit

$$\mathbf{E} = \int \left( \frac{\mathbf{v}^2}{2} + \frac{B^2}{8\pi\rho} \right) dV = \int \left( \frac{z^{+2} + z^{-2}}{4} \right) dV$$

Cross helicity

$$\mathbf{H}_c = \int (\mathbf{v} \cdot \mathbf{B}) dV$$

Energy and cross helicity conservation is equivalent to **pseudo energies** conservation

Pseudoenergies:

$$\mathbf{E}^\sigma = \int \frac{z^{\sigma 2}}{2} dV$$

for  $\sigma = +1, -1$

In **3D** magnetic helicity is also invariant

$$\mathbf{H}_m = \int (\mathbf{A} \cdot \mathbf{B}) dV$$

In **2D** the third invariant is

$$\mathbf{H} = \int |\mathbf{A}|^2 dV$$



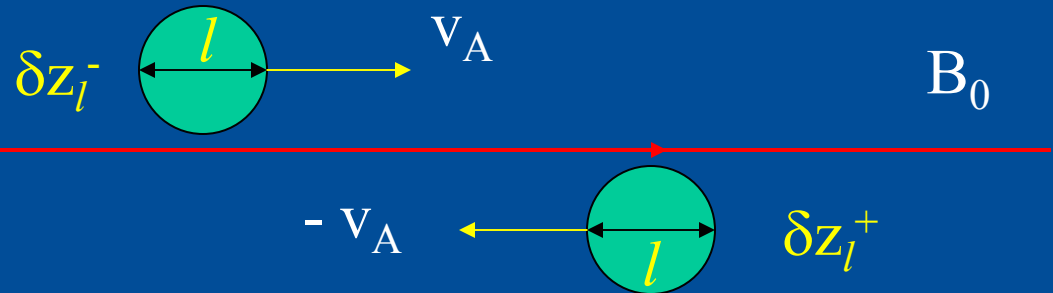
# Non linear MHD cascade 1



Both pseudoenergies are conserved in the NL cascade along the spectrum

$$\Pi_l^\sigma \sim \frac{\delta z_l^{\sigma 2}}{T_l^\sigma} \sim \varepsilon^\sigma$$

**Alfven effect:** interacting eddies move in opposite directions in a large scale magnetic field



Interaction stops after a time  $\tau_l^A \sim l / v_A$

After  $N$  uncorrelated interactions, i.e. after a time  $T_l \sim N \tau_l^A$

$$\Delta z_l^\sigma \sim \sqrt{N} \frac{\delta z_l^{-\sigma} \delta z_l^\sigma}{l} \tau_l^A$$

A significant variation of  $\delta z_l^\sigma$  requires  $\delta z_l^\sigma \sim \Delta z_l^\sigma$  thus

$$N \sim \left( \frac{v_A}{\delta z_l^{-\sigma}} \right)^2 \gg 1 \quad \longrightarrow \quad T_l^\sigma \sim \left( \frac{v_A}{\delta z_l^{-\sigma}} \right)^2 \frac{l}{v_A}$$

# Non linear MHD cascade 2



The energy flow along the spectrum is independent of  $\sigma$

$$\Pi_l^\sigma \sim \frac{\delta z_l^{\sigma^2} \delta z_l^{-\sigma^2}}{lv_A} \sim \varepsilon$$

The spectrum is formed when there is a sufficient energy on both modes of propagation, i.e.  $\delta z_l^- \sim \delta z_l^+ \sim \delta z_l$  then

$$\delta z_l \sim \varepsilon^{1/4} v_A^{1/4} l^{1/4}$$



$$E(k) \propto k^{-3/2}$$

Kraichnan's spectrum

After the spectrum formation **pseudoenergies** are transferred along the spectrum (**and dissipated**) at the same rate

$$E^- - E^+ = const$$



$$\int \mathbf{v} \cdot \mathbf{B} dV = const$$

**Cross helicity is conserved while energy is dissipated**

In the final state

$$E^+ = 0$$



$$\delta \mathbf{v} = \frac{\delta \mathbf{B}}{\sqrt{4\pi\rho}}$$

# Fourier analysis in a cubic box



In a periodic cubic box of size  $L$

$$\mathbf{k} = \frac{2\pi}{L} \mathbf{n}$$

$$z_{\alpha}^{\sigma}(\mathbf{r}, t) = \sum_{\mathbf{k}} z_{\alpha}^{\sigma}(\mathbf{k}, t) e^{i\mathbf{k} \cdot \mathbf{r}}$$

$$z_{\alpha}^{\sigma}(\mathbf{k}, t) = L^{-3} \int z_{\alpha}^{\sigma}(\mathbf{r}, t) e^{-i\mathbf{k} \cdot \mathbf{r}} d\mathbf{r}$$

Fourier analysis

Divergenceless condition

3D

2D

$$\mathbf{z}^{\sigma}(\mathbf{k}, t) = \sum_{\alpha=1,2} z_{\alpha}^{\sigma}(\mathbf{k}, t) \mathbf{e}_{\alpha}(\mathbf{k})$$

$$\mathbf{k} \cdot \mathbf{e}_{\alpha}(\mathbf{k}) = 0$$

$$\mathbf{e}_1(\mathbf{k}) = \frac{i\mathbf{k} \times \mathbf{B}_0}{|\mathbf{k} \times \mathbf{B}_0|}; \mathbf{e}_2(\mathbf{k}) = \frac{i\mathbf{k}}{|\mathbf{k}|} \times \mathbf{e}_1(\mathbf{k})$$

$$\mathbf{z}^{\sigma}(\mathbf{k}, t) = z^{\sigma}(\mathbf{k}, t) \mathbf{e}(\mathbf{k})$$

$$\mathbf{k} \cdot \mathbf{e}(\mathbf{k}) = 0$$

# MHD equations for Fourier modes



The evolution of the field for a single wave vector is related to fields of **all** other wave vectors (convolution term) for which  **$\mathbf{k} = \mathbf{p} + \mathbf{q}$** .

$$\left( \frac{\partial}{\partial t} - i\sigma \mathbf{k} \cdot \mathbf{v}_A + \nu k^2 \right) z_\alpha^\sigma(\mathbf{k}, t) = \sum_{\beta, \gamma=1}^2 \sum_{\mathbf{p}+\mathbf{q}=\mathbf{k}} M_{\alpha\beta\gamma}(\mathbf{k}, \mathbf{p}, \mathbf{q}) z_\gamma^\sigma(\mathbf{p}, t) z^{-\sigma}(\mathbf{q}, t)$$

where

$$M_{\alpha\beta\gamma}(\mathbf{k}, \mathbf{p}, \mathbf{q}) = (i\mathbf{k} \cdot \mathbf{e}_\gamma(\mathbf{q})) (\mathbf{e}_\alpha^*(\mathbf{p}) \cdot \mathbf{e}_\beta(\mathbf{q}))$$

Infinite number of modes involved in nonlinear interactions for inviscid flows

# Direct numerical simulations 1



## Pseudospectral methods:

- Time integration in Fourier space;
- Non linear terms evaluated in physical space;
- From Fourier space to physical space and viceversa Fast Fourier transforms (FFT) are used.

## From phenomenological arguments:

$$\frac{k_D}{k_I} \sim \text{Re}^{3/4}$$

## High performance computers:

- 2D             $\text{Re} \sim 10^4$
- 3D             $\text{Re} \sim 10^3$

# Direct numerical simulations 2



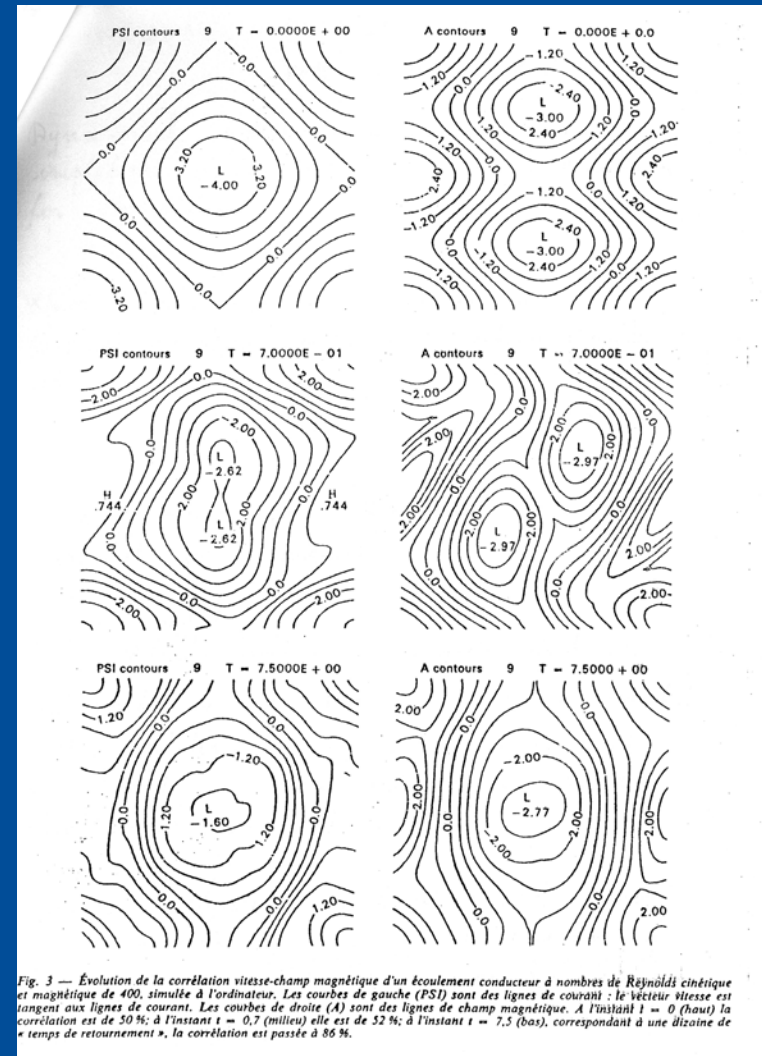
From Grappin, 1986

Velocity field  
lines

Magnetic field  
lines

Velocity and  
magnetic field lines  
are parallel in the  
final state

Growth of  $v - B$   
correlation



Time evolution

# Dynamical (shell) models 1

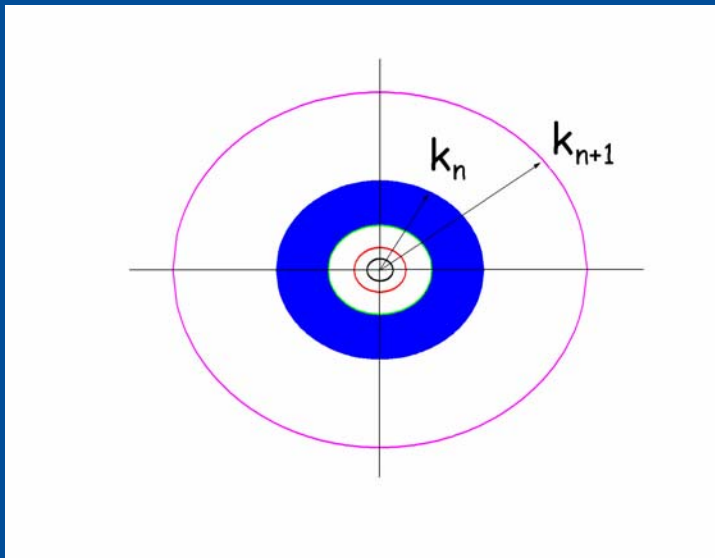


Shell models are dynamical models representing a simplified version of the spectral equations for turbulence

## Step 1

Introduce a logarithmic spacing in the wave vectors space (shells)

$$k_n = k_0 \lambda^n$$
$$n = 1, 2, \dots, N$$



The intershell ratio in general is set equal to  $\lambda = 2$ .

We are not interested in the dynamics of each wave vector mode of Fourier expansion, rather in the gross properties of dynamics at small scales.

In this way we can investigate properties of turbulence at very high Reynolds numbers.

# Dynamical (shell) models 2



## Step 2

Assign to each shell **ONLY** two dynamical variables

$$z_n^\pm(t) = u_n(t) \pm b_n(t)$$

The possibility to investigate both spatial and temporal properties of turbulence is ruled out

Velocity field

Magnetic field

These fields take into account the averaged effects of velocity modes between  $k_n$  and  $k_{n+1}$ , that is fluctuations across eddies at the scale  $r_n \sim k_n^{-1}$

## Step 3

Write quadratic NL equations for these variables where only nearest and next nearest coupling interactions are retained

$$\frac{dz_n^\sigma(t)}{dt} = ik_n \sum_{i,j=\pm 2,\pm 1} M_{i,j} z_{n+i}^\sigma(t) z_{n+j}^{-\sigma}(t)$$



# Dynamical (shell) models 3



## Step 4

Fix the coupling coefficients  $M_{ij}$  imposing the conservation of ideal quadratic invariants (energy, cross helicity, magnetic helicity)

$$\frac{du_n}{dt} + \nu k^2 u_n = ik_n [(u_{n+1} u_{n+2} - b_{n+1} b_{n+2}) - \frac{1}{4} (u_{n-1} u_{n+1} - b_{n-1} b_{n+1}) - \frac{1}{8} (u_{n-2} u_{n-1} - b_{n-2} b_{n-1})]^* + f_n$$

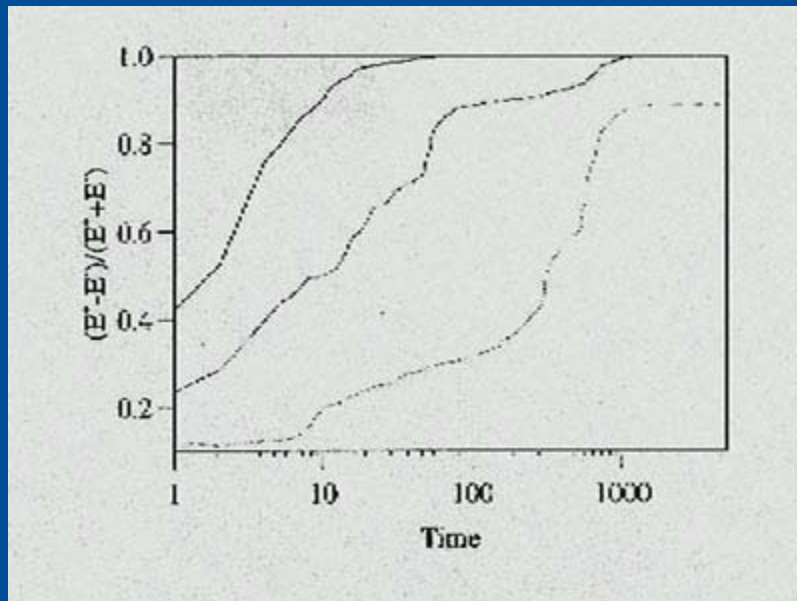
$$\frac{db_n}{dt} + \eta k^2 b_n = ik_n \frac{1}{6} [(u_{n+1} b_{n+2} - b_{n+1} u_{n+2}) - (u_{n-1} b_{n+1} - b_{n-1} u_{n+1}) + (u_{n-2} b_{n-1} - b_{n-2} u_{n-1})]^* + g_n$$

Forcing terms

# Dynamical alignment in shell models



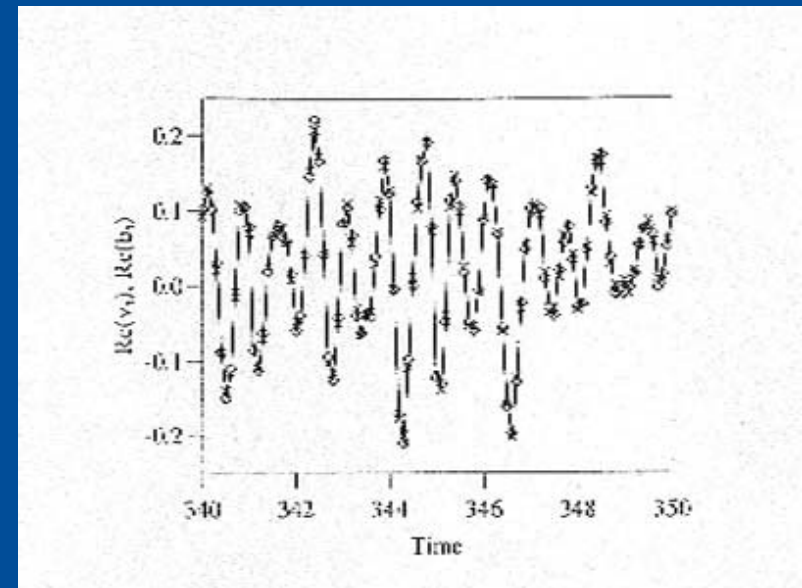
## A decay simulation



The cross helicity to energy ratio grows in time

## A forced simulation:

Time evolution of mode  $n = 7$ , with constant forcing terms.

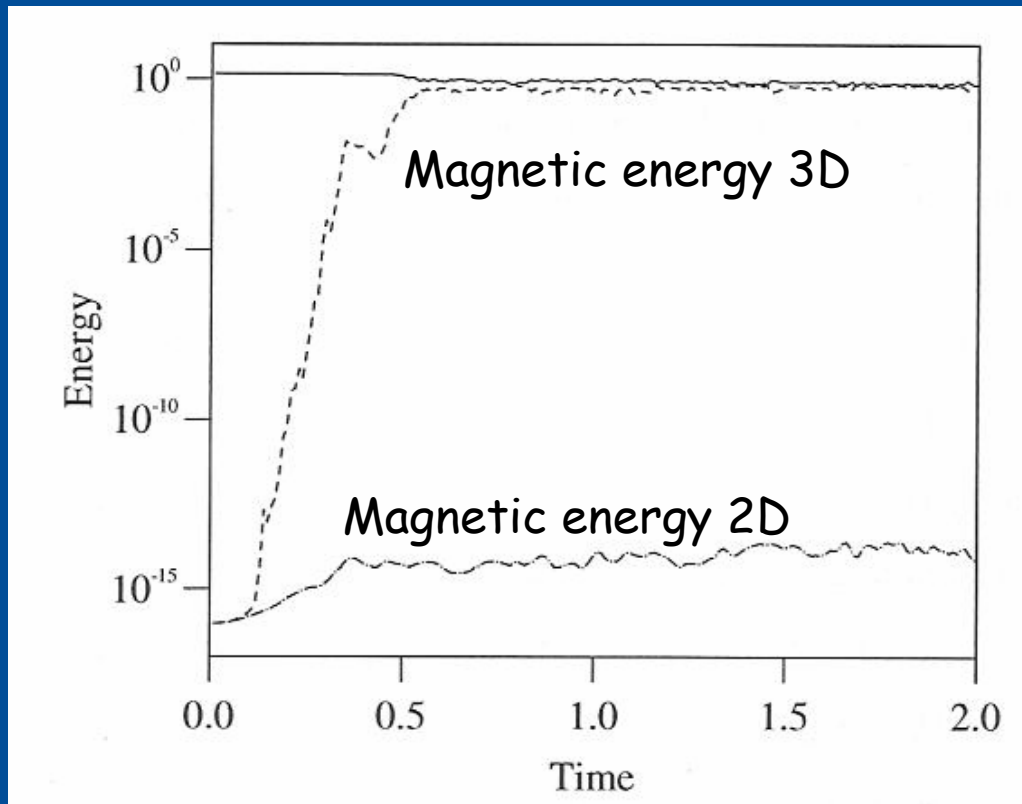


Velocity (diamonds) and magnetic field (crosses) amplitudes strongly correlated

# Dynamo action in shell models



## What "turbulent dynamo action" means in the shell model



There exists some "invariant subspaces" which can act like "attractors" for all solutions (stable subspaces).

The fluid subspace is stable (in 2D case) or unstable (in 3D case).

The structure of stable and unstable time-invariant subspaces of real MHD are reproduced in the shell models

# Alfvenic correlation: a different scenario 1



**Alfvenic states**, i.e. states of high correlation between velocity and magnetic field fluctuations are spontaneously formed in MHD turbulence

**Solar wind turbulence evolves in the reverse way:**

- Highly correlated near the sun up to 1 AU
- At larger radial distances from 1 AU to 10 AU:
  - Correlation is progressively lowered
  - Level of compressive  $\delta r$ ,  $\delta|B|$  fluctuations progressively increased

Possible solution to such paradox:

Solar wind is neither incompressible nor statistically homogeneous

# Alfvenic correlation: a different scenario 2



Commonly accepted scenario:

- Main source of fluctuations inside the critical point (solar photosphere)
- Critical point filters out inward propagating waves, only outward propagating Alven waves arrive in the solar wind

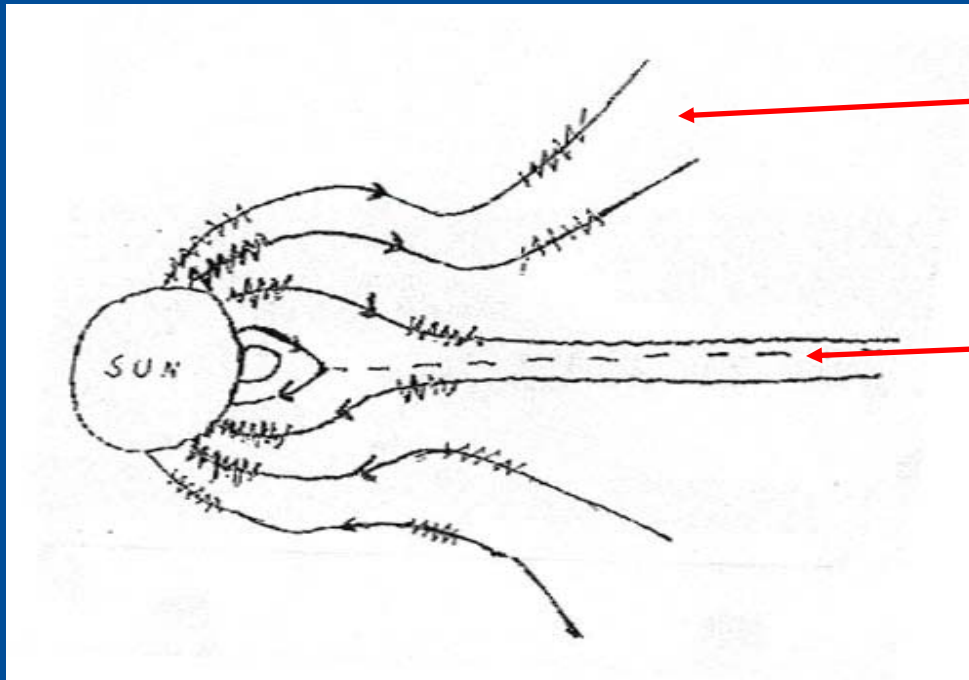
Large amplitudes Alfven waves generated at the foot points of open magnetic field lines

- either converge towards the heliospheric current sheet (slow wind)
- or propagate in the fast solar wind

# Alfvenic correlation: a different scenario 3



Two interesting physical problems



Fast wind

Slow wind:  
current sheet

Large amplitude **Alfven waves** converging on the current sheet **interact** with the associated large scale **inhomogeneity**

Large amplitude **Alfven waves** propagating in fast wind could be subject to **parametric instability**

# Turbulence in the heliospheric current sheet 1



Space observations close to the heliospheric **current sheet**:

- depletion of  $\delta v - \delta B$  correlation
- higher level of compressive  $\delta n, \delta |B|$  fluctuations
- Kolmogorov - like spectra for  $v, B, n, |B|$

**Numerical simulations** to study compressive effects (Malara et al., 1996, 1997)

## **Model:**

- A large scale current sheet
- An initial alfvénic perturbation (outward propagating waves on both sides of the current sheet)
- An initial uniform  $|B| = |B_{eq} + \delta B|$  (no initial ponderomotive force)

# Turbulence in the heliospheric current sheet 2



Model equations:

$$\frac{\partial \rho}{\partial \tau} + \nabla \cdot (\rho \mathbf{v}) = 0$$

$$\frac{\partial \mathbf{v}}{\partial \tau} + (\mathbf{v} \cdot \nabla) \mathbf{v} = -\frac{1}{\rho} \nabla (\rho T) + \frac{1}{\rho} (\nabla \times \mathbf{b}) \times \mathbf{b} + \frac{1}{\rho S_\nu} \nabla^2 \mathbf{v}$$

$$\frac{\partial \mathbf{b}}{\partial \tau} = \nabla \times (\mathbf{v} \times \mathbf{b}) + \frac{1}{S_\eta} \nabla^2 \mathbf{b}$$

$$\frac{\partial T}{\partial \tau} + (\mathbf{v} \cdot \nabla) T + (\gamma - 1) T (\nabla \cdot \mathbf{v}) = \frac{\gamma - 1}{\rho} \left[ \frac{1}{S_\kappa} \nabla^2 T + \frac{1}{S_\nu} \left( \frac{\partial v_i}{\partial x_j} \frac{\partial v_i}{\partial x_j} \right) + \frac{1}{S_\eta} (\nabla \times \mathbf{b})^2 \right]$$

**Numerical method:**

- 2-1/2 D code
- Pseudospectral: Fourier in the homogeneity direction, Chebshev across the current sheet
- Multidomain: a matching performed to increase resolution inside the current sheet



# Turbulence in the heliospheric current sheet 3



Initial conditions:

Magnetic field

$$\mathbf{b}(x, y, 0) = A \left\{ \varepsilon \cos[\phi(y)] \mathbf{e}_x + \sin(\alpha) F(x) \mathbf{e}_y + \sqrt{1 - \sin^2(\alpha) F^2(x) + \varepsilon^2 \sin^2[\phi(y)]} \mathbf{e}_z \right\}$$

Velocity field

$$\mathbf{v}(x, y, 0) = \sigma(x) \frac{\delta \mathbf{b}(x, y, 0)}{\sqrt{\rho(x, y, 0)}}$$

Density and temperature

$$\rho(x, y, 0) = 1 \quad \text{and} \quad T(x, y, 0) = T_0$$

Where  $\varepsilon = 0.5$ ,

$$F(x) = \tanh(x) \quad \text{and}$$

$$\phi(y) = 2 \sum_{m=1}^{m_{\max}} (mk_0)^{-5/3} (\cos mk_0)$$

The equilibrium magnetic field  $\mathbf{B}_{eq}$  is obtained by setting  $\varepsilon = 0$  and rotates by an angle  $\alpha$  in the plane  $yz$

# Turbulence in the heliospheric current sheet 4



The initial correlation between  $\delta\mathbf{v}$  and  $\delta\mathbf{B}$  is strongly reduced in the current sheet region

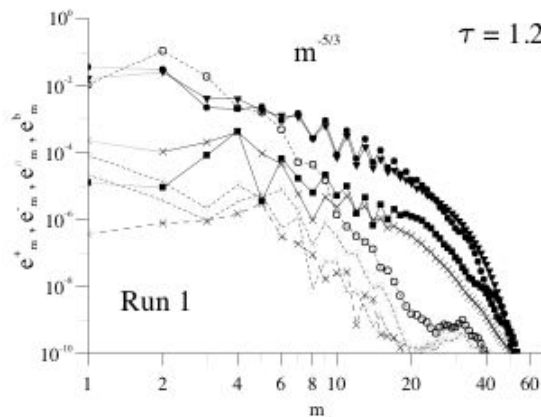
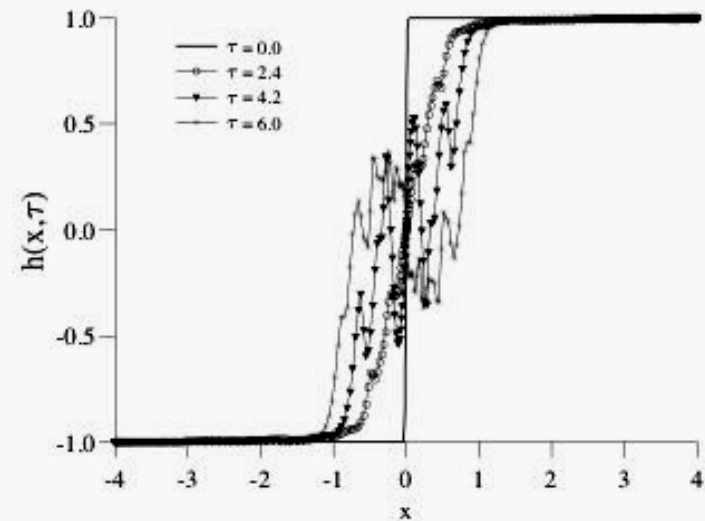


Fig. 3. The Fourier spectra of pseudoenergies fluctuation  $e_m^+(x, \tau)$  (circles),  $e_m^-(x, \tau)$  (triangles), density fluctuation  $e_m^\rho$  (squares) and magnetic field intensity fluctuation  $e_m^B$  (crosses) are represented as functions of the wavenumbers at  $x = 0.2$  (full lines) and at  $x = 3.01$  (dashed lines) at the time  $\tau = 1.2$ , for  $\beta = 0.2$

Compressible fluctuations  $\delta\rho$  and  $\delta|\mathbf{B}|$  are generated

Inside neutral sheet the spectra for  $E^+$ ,  $E^-$  and  $\delta\rho$  are superposed.

The spectral index is  $5/3$ .

# Density magnetic field intensity correlation 1

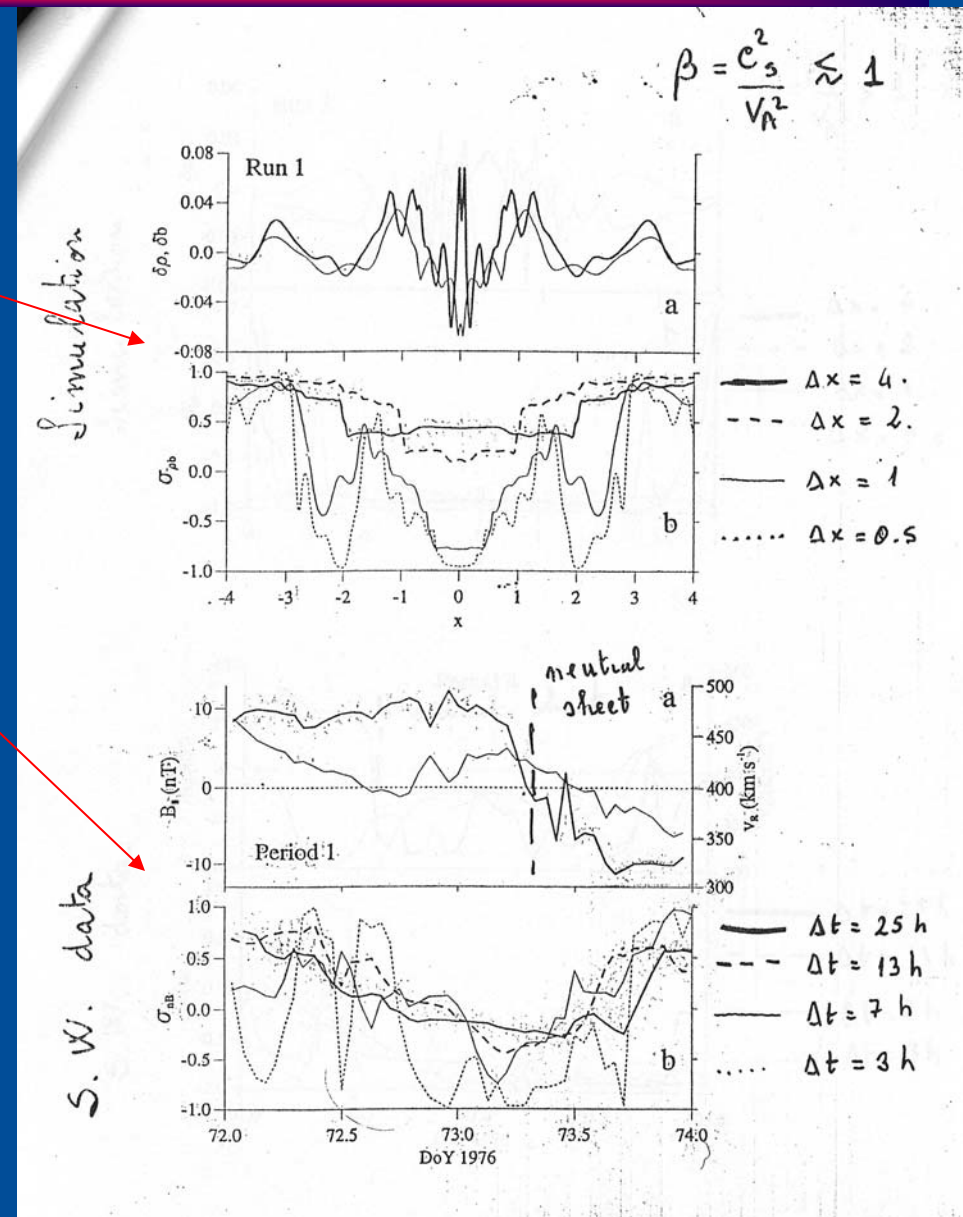


Simulation **vs** solar wind data analysis

For  $\beta < 1$

$\delta\rho$  and  $\delta|B|$ :

- anticorrelated at small scales inside current sheet (slow mode fluctuations)
- correlated at large scale outside the current sheet (fast mode fluctuations)



# Density magnetic field intensity correlation 2

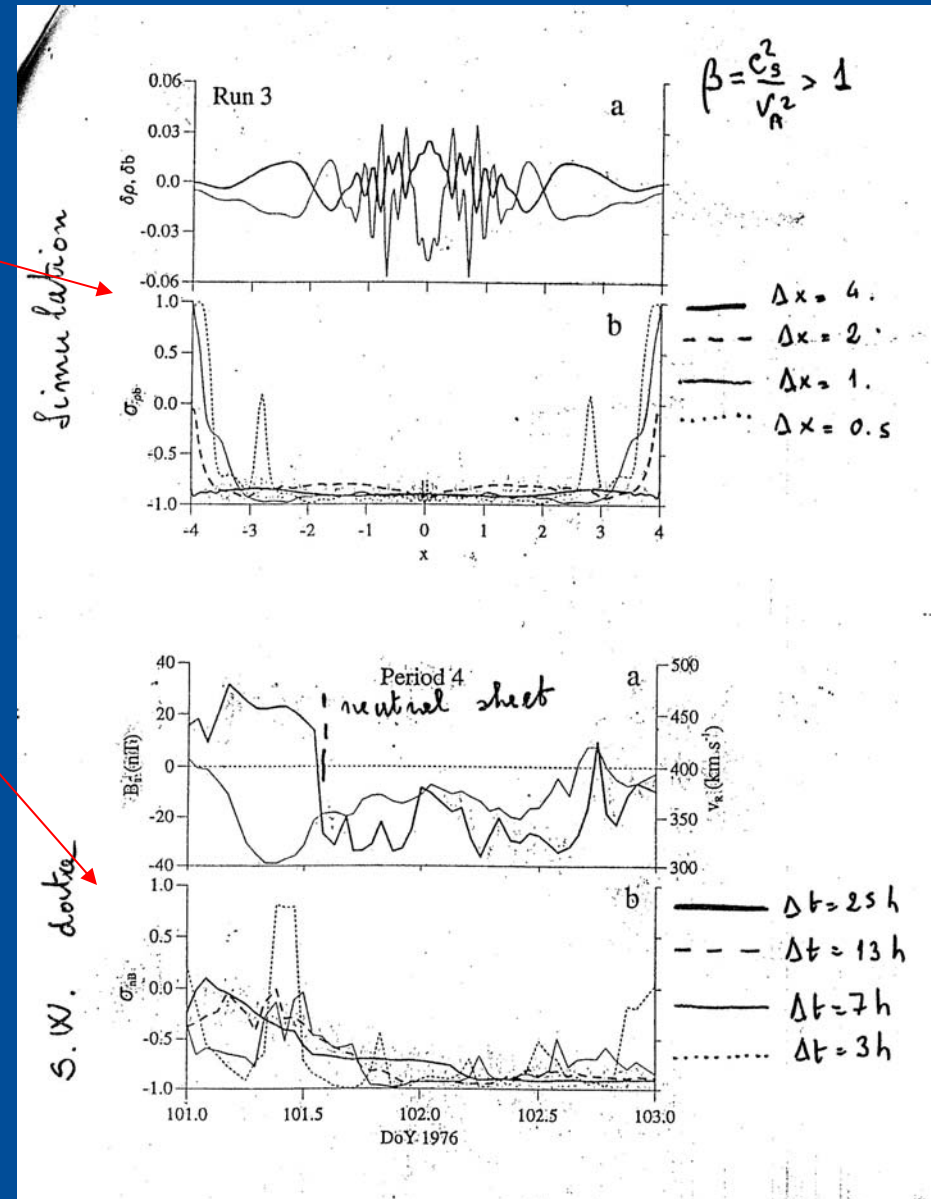


Simulation **vs** solar wind data analysis

For  $\beta > 1$

$\delta\rho$  and  $\delta|B|$ :

➤ anticorrelated at all scales and almost everywhere (slow mode fluctuations)



# Density Temperature fluctuation correlation 1



At small scale  $\delta\rho - \delta T$  correlation mainly positive in the fast streams while it displays both signs in slow streams (Bavassano et al., 1995):

where does the negative correlation come from ?

In an ideal fluid entropy  $S$  is advected by velocity field like a passive scalar

$$\left[ \frac{\partial}{\partial t} + \mathbf{v} \cdot \nabla \right] S = 0$$

$S$  initially uniform

- isentropic flow
- polytropic equation of state
- only positive correlation are allowed

$$\frac{T}{\rho^{\gamma-1}} = \text{const}$$
$$\frac{\delta T}{T} = (\gamma - 1) \frac{\delta\rho}{\rho}$$

Small amplitude modes:

both fast and slow modes display  $\delta\rho - \delta T$  positively correlated

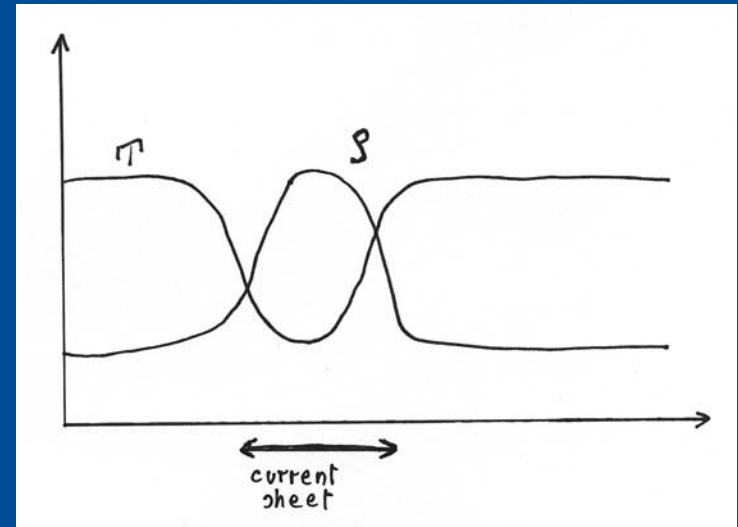
# Density Temperature fluctuation correlation 2



Zank and Matthaeus 1991, 1993:  
heat conduction term allows for a negative correlation  
also in a statistically homogeneous configuration (Nearly  
Incompressible MHD approach)

Malara et al., 1998:  
Large scale ( $\sim 1$  day) variations  
of **density** and **temperature**  
furnish a reservoir of entropy  
fluctuations

$$S \propto \ln\left(\frac{T}{\rho^{\gamma-1}}\right)$$



Plasma turbulence can mix **S**, moving the **S** modulation from large  
to small scales (small amplitude entropy waves display negative  
 $\delta\rho - \delta T$  correlations)

# Density Temperature fluctuation correlation 3



The sign of  $\delta\rho - \delta T$  correlation results from competition between :

- production of magnetosonic compressive fluctuations  $\langle \delta\rho \delta T \rangle > 0$
- entropy cascade  $\langle \delta\rho \delta T \rangle < 0$

Numerical model (Malara et al., 1998) :

- Large scale current sheet
- Density and temperature large scale modulation

Initial conditions:

$$\rho(x, y, t = 0) = \rho_0 \left\{ 1 + \Delta \left[ \frac{1}{\cosh^2(x/a_e)} + p \left( \frac{x}{a_e} \right)^2 \right] \right\}$$

$$T(x, y, t = 0) = \rho_0 T_0 / \rho(x, y, t = 0)$$

Pressure and magnetic field intensity are constant

# Density Temperature fluctuation correlation 4

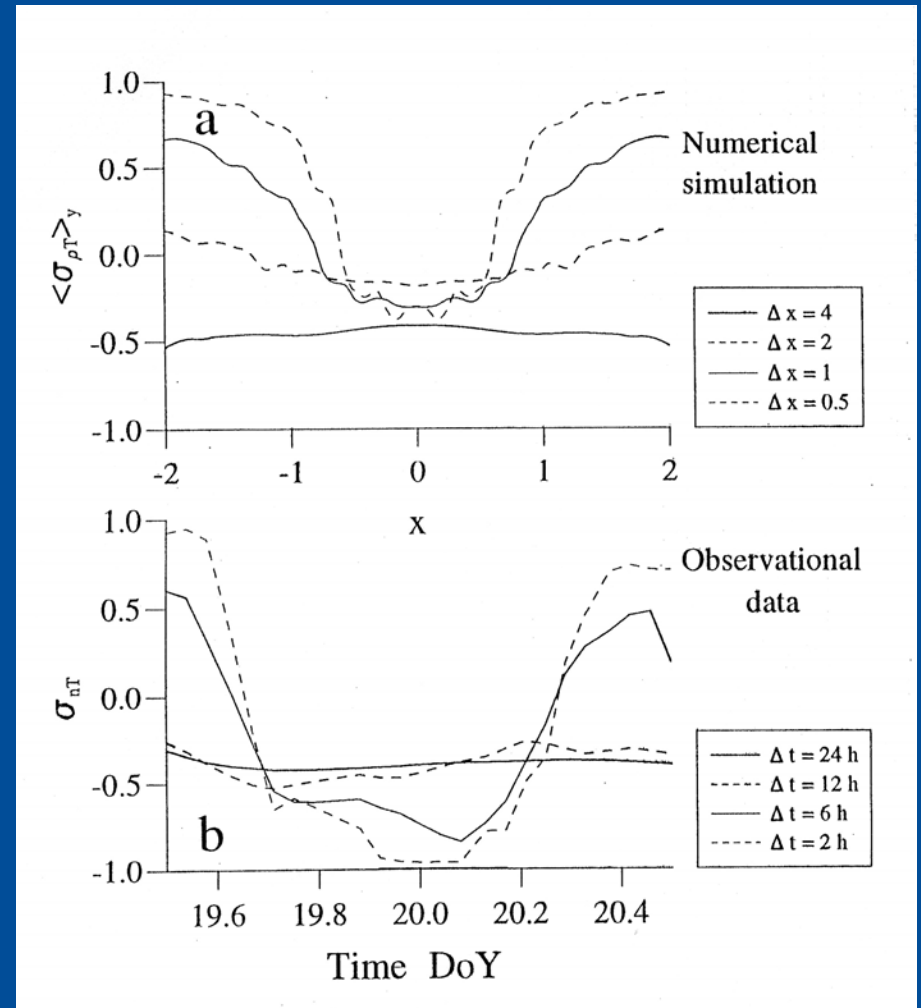


Pierluigi Veltri  
Dipartimento di Fisica, Università della Calabria

At large scales  $\langle \delta\rho \delta T \rangle < 0$   
in the whole domain

At small scales

- $\langle \delta\rho \delta T \rangle < 0$  in the current sheet
- NL interactions more effective inside current sheet where entropy cascade prevails
- $\langle \delta\rho \delta T \rangle > 0$  outside the current sheet (fast magnetosonic fluctuations propagate outside)





# Parametric Instability of Alfvénic fluctuations 1



Fast speed stream and polar wind much more homogeneous than current sheet region, but  $E^+/E^-$  increases with the distance from the sun;  
can parametric instability be responsible for this ?

Mother coherent Alfvén wave decays in

- an Alfvén wave propagating in the opposite direction
- a sound wave

What happens when starting with a broad band initial wave ?

Non linear numerical investigation of evolution of **initial conditions**

$$\delta \mathbf{B} = B_1 [\cos(\phi(x)) \mathbf{e}_y + \sin(\phi(x)) \mathbf{e}_z]$$

$$\delta \mathbf{v} = -\frac{v_A}{B_0} \delta \mathbf{B}$$

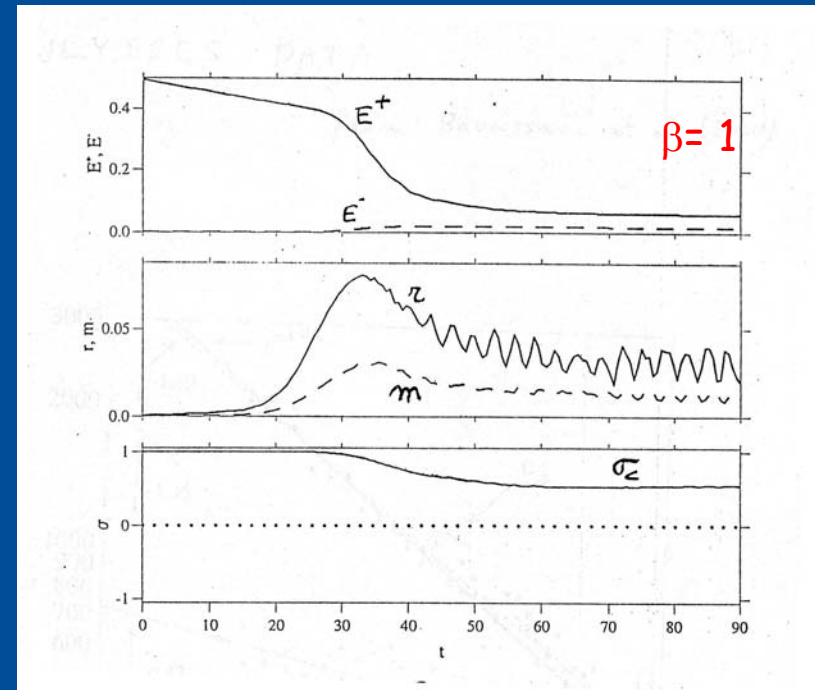
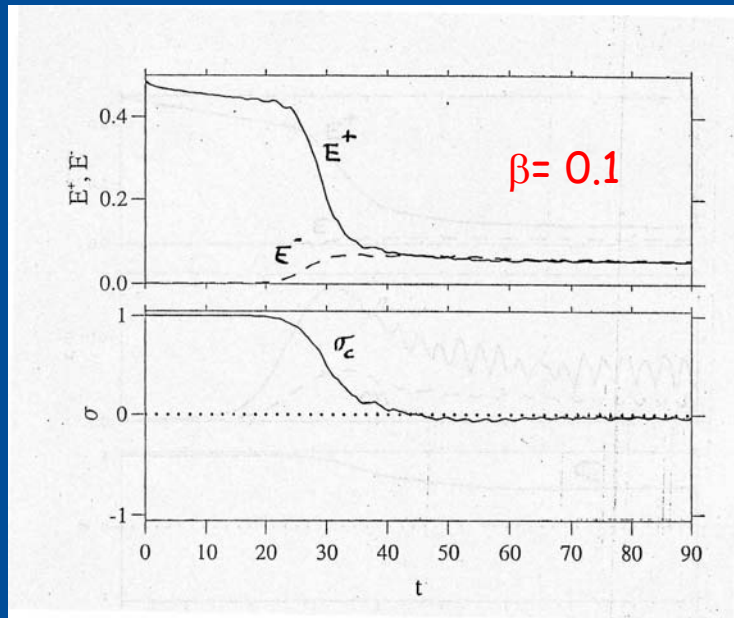
with

$$\phi(x) = k_0 x + a \sum_{n=-N}^N |n|^{-\alpha} e^{in(x+\delta)}$$

# Parametric Instability of Alfvénic fluctuations 2



Simulation results:



Inward propagating Alfvén wave, density and magnetic field intensity fluctuations all grow in time

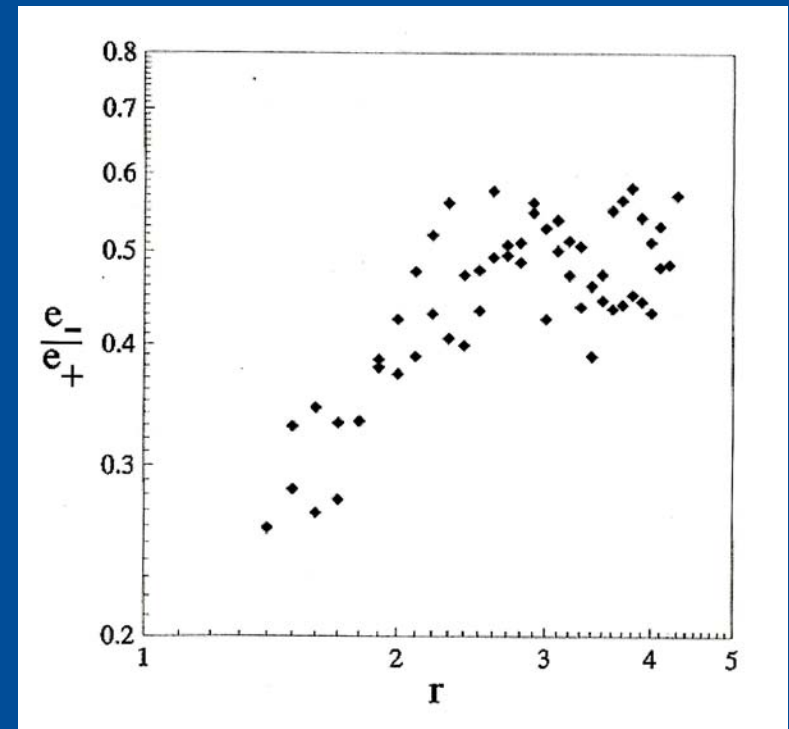
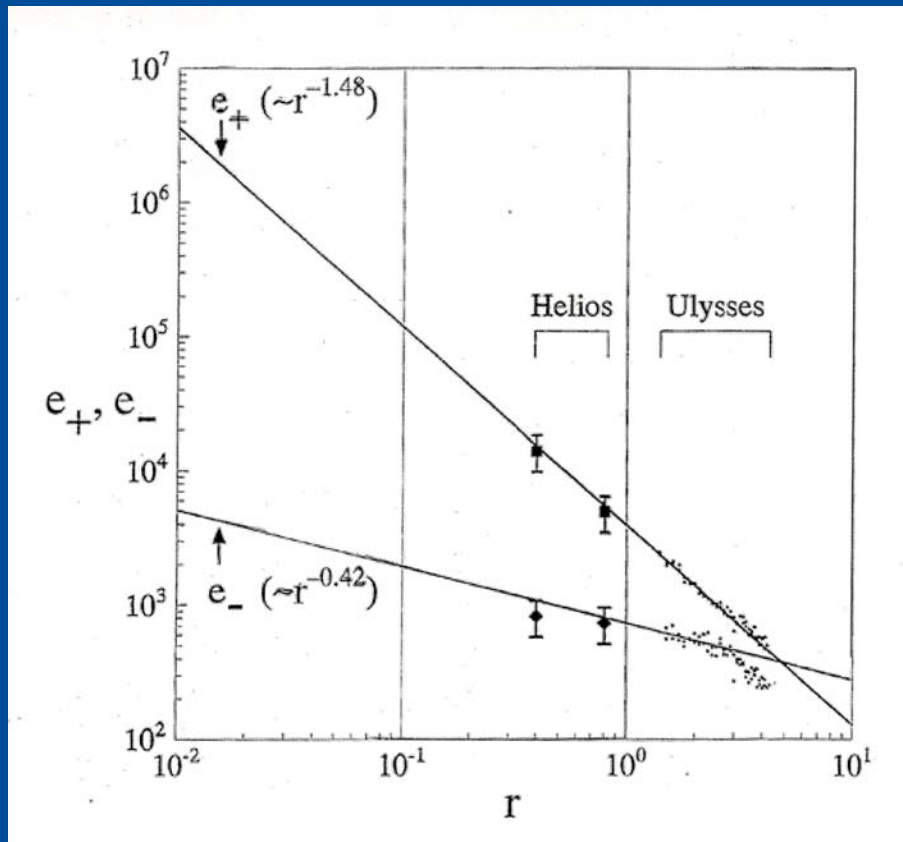
At instability **saturation**;

- for small  $\beta$ ,  $E^-$  grows to the same level as  $E^+$
- for intermediate  $\beta$ ,  $E^-$  level grows but it remains lower than  $E^+$ , the parametric process is unable to completely destroy  $v - B$  correlation

# Parametric Instability of Alfvénic fluctuations 3



Pierluigi Veltri  
Dipartimento di Fisica, Università della Calabria



Bavassano et al., 2000

Data analysis: saturation seems to occur at 2.2 AU radial distance at a level  $E_-/E_+ \sim 0.5$

Trieste  
2003

# Parametric Instability of Alfvénic fluctuations 4

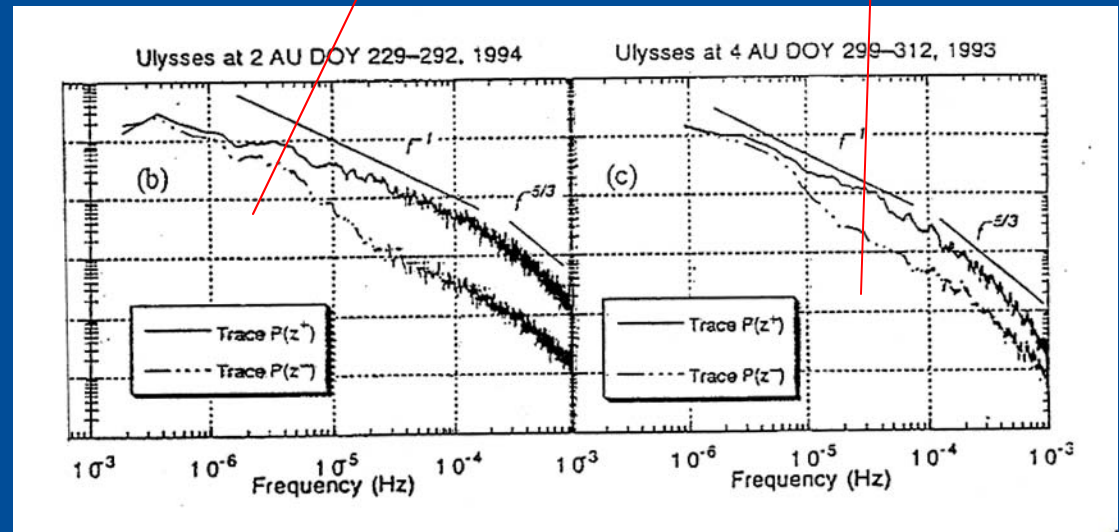
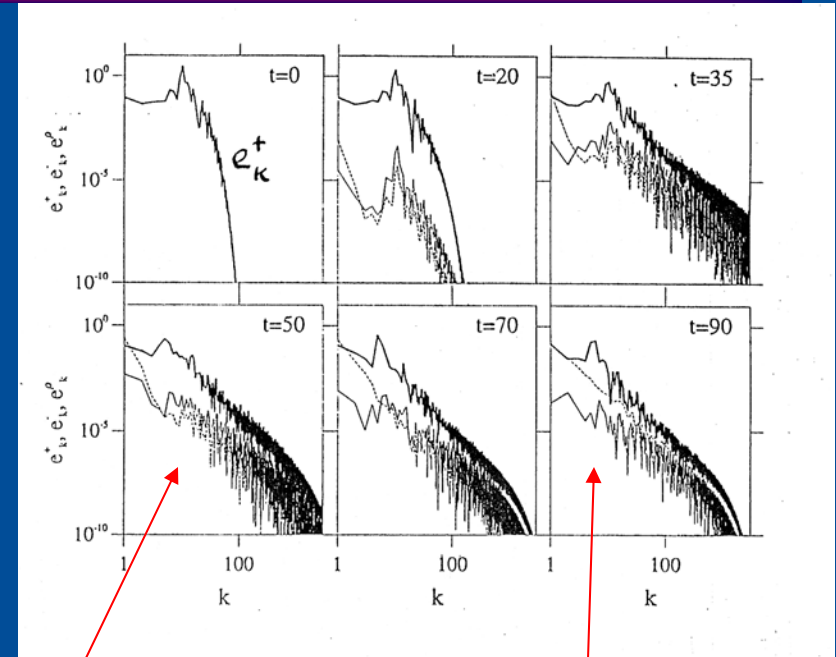


Pierluigi Veltri  
Dipartimento di Fisica, Università della Calabria

## Spectra:

- Both direct and inverse cascades are observed
- At large and small scales  $E^+$  and  $E^-$  spectra finally superpose
- At intermediate scales  $E^+$  still dominates
- The spectral index of  $E^+$  progressively decreases and approaches  $5/3$

---  $E^-(k)$   
—  $\rho(k)$



# Conclusions

Analysis of space data has stimulated a lot of theoretical work devoted to understand the observed properties of MHD turbulence

Numerical simulations are able to explain several observed features of MHD turbulence in solar wind.

In slow wind the interaction of Alfvén waves with Heliospheric current sheet produces:

- The depletion of Alfvénic correlation
- The generation of compressive fluctuations
- The spectral features of fluctuations
- The behavior of both  $r - |B|$  and  $r - T$  fluctuation correlations

In fast wind parametric instability allows to understand

- The time evolution of Alfvénic fluctuations
- The spectral features of both Alfvénic and compressive fluctuations generated

# MHD Turbulence in heliospheric plasma: Intermittency and small scale structures

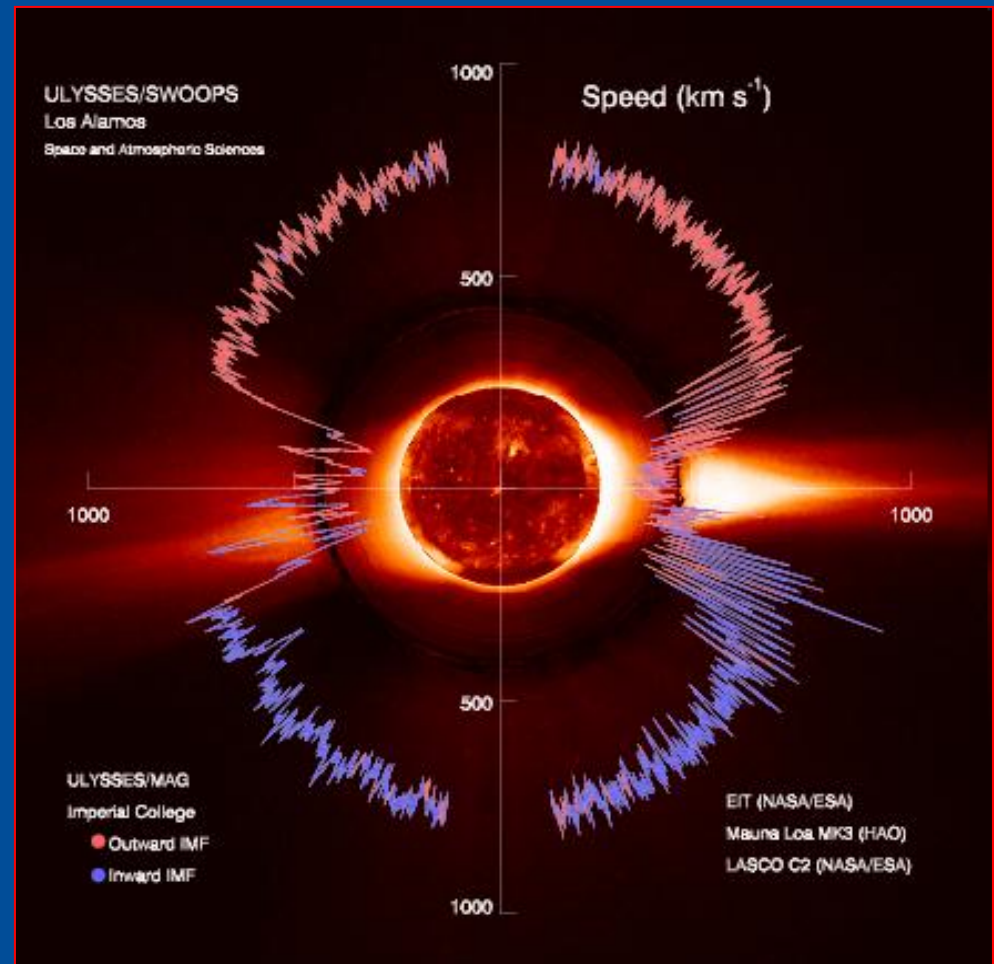


Pierluigi Veltini  
Dipartimento di Fisica, Università della Calabria

Solar wind: a wind tunnel  
Supersonic and  
superalfvenic flow  
 $250 \text{ Km/s} < V_{sw} < 800 \text{ Km/s}$

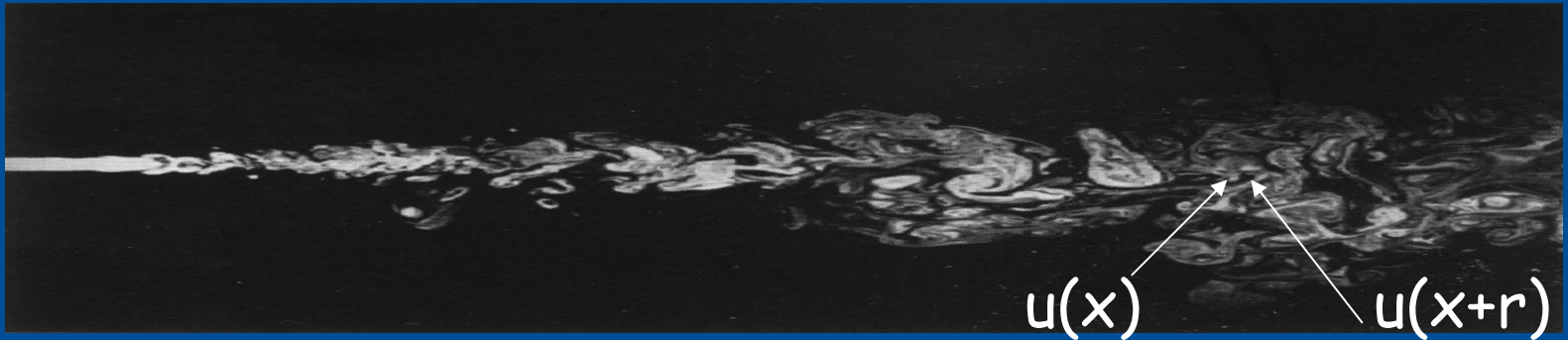
In situ measurements of  
high amplitude fluctuations  
of velocity and magnetic  
fields over 6 decades of  
frequencies (up to ion  
cyclotron frequency)

$$10^{-6} \text{ Hz} < f < 1 \text{ Hz}$$



From Taylor hypothesis:  $L \sim V_{sw} / f$  Scale range  $400 \text{ Km} < L < 1 \text{ AU}$

# Two-points correlation : higher order moments



$$\delta u_r(x) = u(x+r) - u(x)$$

**Gaussian process:** the 2-th order moment is sufficient to fully determine probability density functions (pdf). High-order moments are uniquely defined from the 2-th order (in this sense energy spectra are interesting!)

High-order moments of two-points differences are probes for non-gaussian behaviour of fluctuations

$$S_n(r) = \langle [\delta u_r(x)]^n \rangle \approx r^{\zeta_n}$$

**Kolmogorov's standard turbulence:**

$$\zeta_n = n/3 \Rightarrow E(k) \approx k^{-5/3}$$

# Self-similarity of fluctuations



Non linear cascade =  
self similar (fractal) process



Pdf for fluctuations should be  
invariant under a scale change

$$P_r(\delta u_r) = r^{-1/3} F\left(\frac{\delta u_r}{r^{-1/3}}\right)$$

Higher order moments: probes of  
self similarity

$$\begin{aligned} S_n(r) &= \int_{-\infty}^{\infty} (\delta u_r)^n P(\delta u_r) d(\delta u_r) = \\ &= r^{n/3} \int_{-\infty}^{\infty} \left(\frac{\delta u_r}{r^{1/3}}\right)^n P\left(\frac{\delta u_r}{r^{1/3}}\right) d\left(\frac{\delta u_r}{r^{1/3}}\right) = A_n r^{n/3} \end{aligned}$$



# Self-similarity of fluctuations



Fluctuations are stochastic variables, high-order moments can be defined in terms of pdfs:

$$S_n(r) = \int_{-\infty}^{\infty} (\delta u_r)^n p(\delta u_r) d\delta u_r$$

Anomalous scaling exponents  $\rightarrow$  pdfs have also anomalous scalings

$$\delta w_r = \frac{\delta u_r}{\langle (\delta u_r)^2 \rangle^{1/2}}$$

$$\delta u_r = u(x+r) - u(x)$$

Changing the scale  $r \rightarrow \lambda r$ , it can be shown that, in a pure fractal situation, pdfs at two scales are related

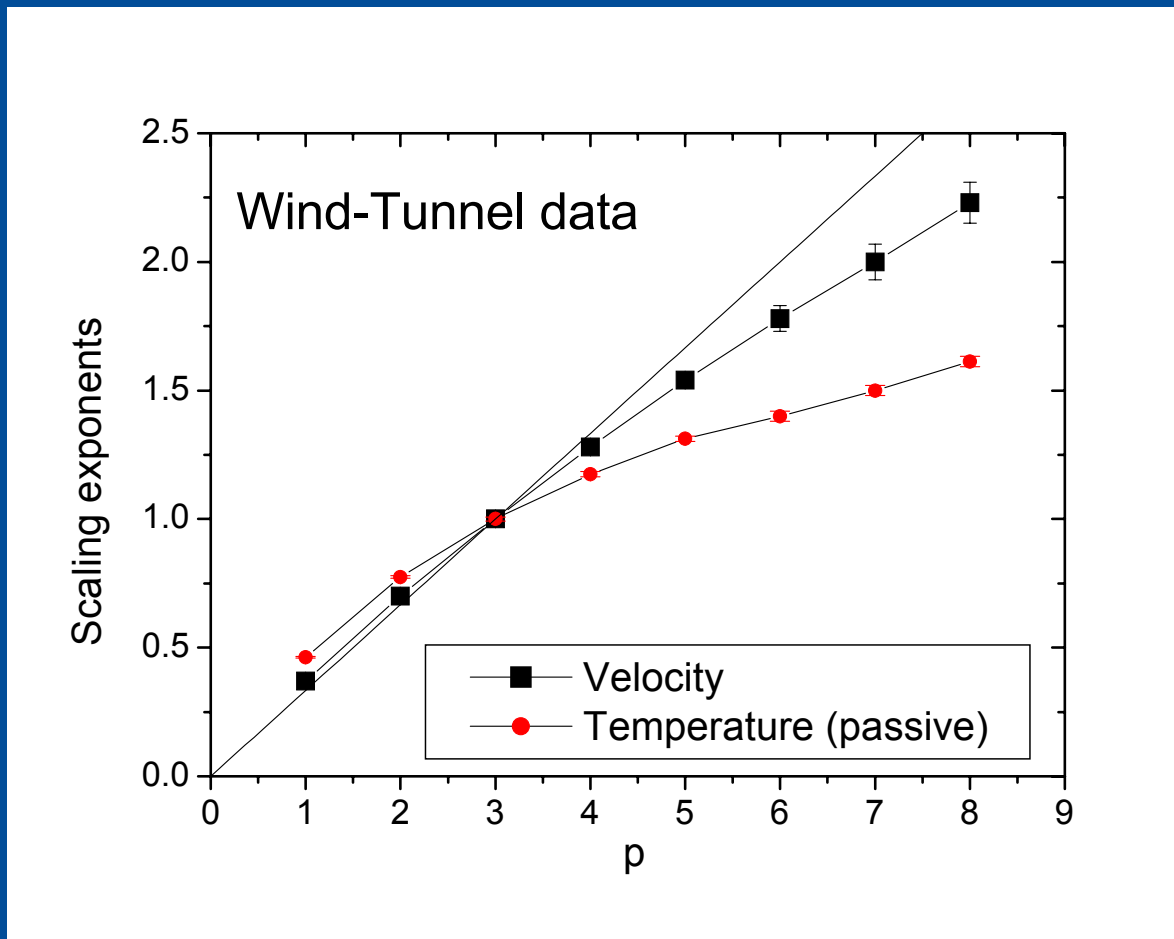
$$pdf(\delta w_{\lambda r}) = pdf(\delta w_r)$$

*i.e.* the pdfs of normalized fields increments at different scales collapse on the same shape (self-similarity)

# Departure from Kolmogorov's scaling



The departure is **SIGNIFICANT**, and has been attributed to **INTERMITTENCY** in fully developed turbulence



The temperature field (passive), is different from velocity field.

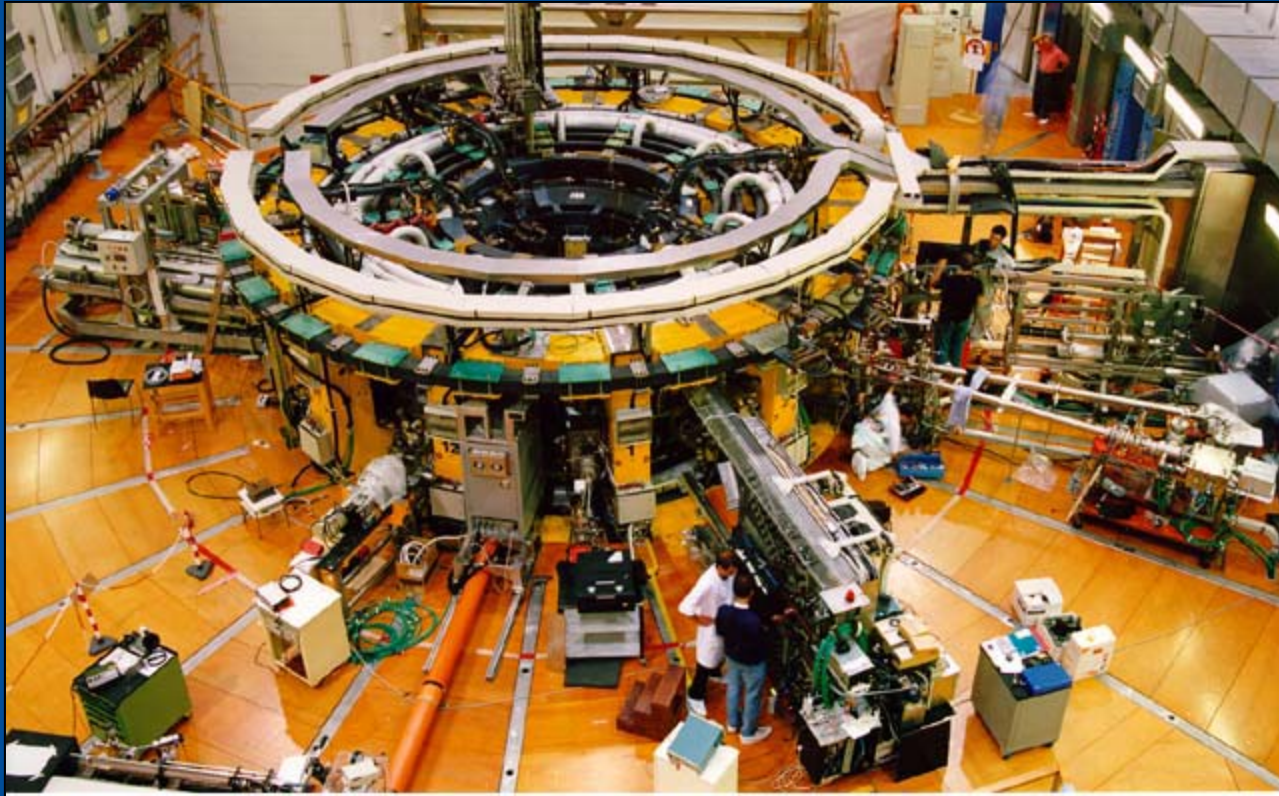


Intermittency (measured as the difference between the actual scaling exponent and the Kolmogorov's law), is stronger for passive scalar

# Laboratory data



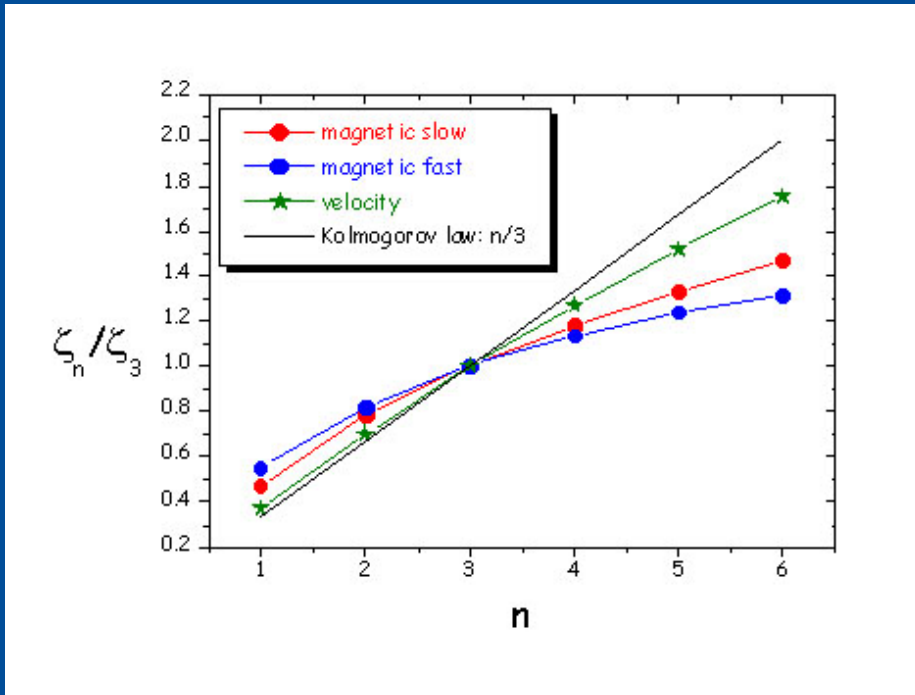
Pierluigi Veltri  
Dipartimento di Fisica, Università della Calabria



Plasma generated for nuclear fusion, confined in a Reversed Field Pinch configuration (RFX, Padua).  
High amplitude fluctuations of magnetic field and floating potential measured at the edge of the device.

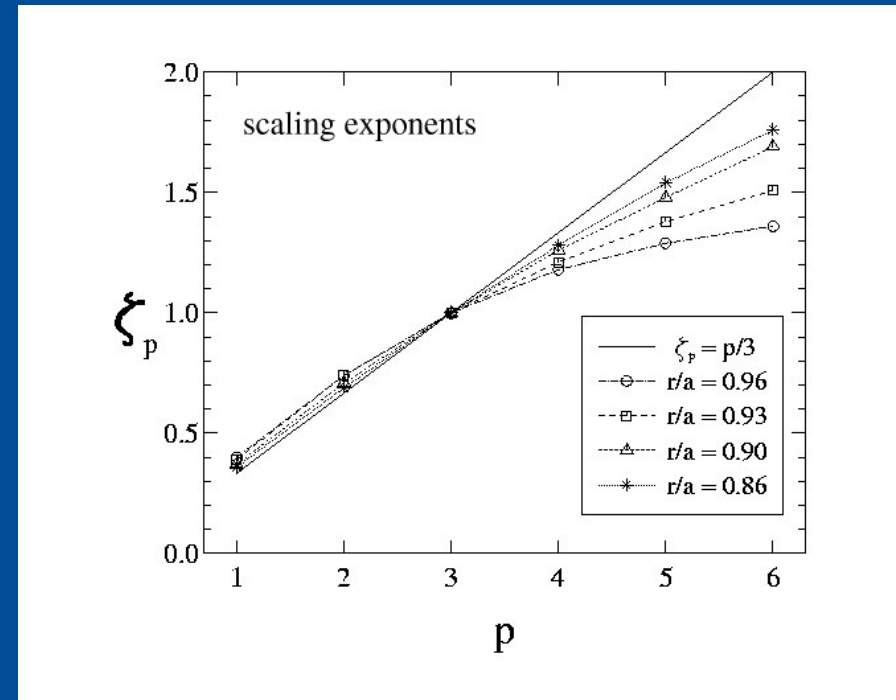
Trieste  
2003

# Anomalous scalings in plasmas turbulence



## Solar wind

Intermittency is stronger for magnetic field than for velocity (magnetic field like a "passive vector" ?)



## Laboratory plasma

Intermittency for magnetic turbulence is stronger near the wall

# Departure from self-similarity



Anomalous scalings  $\rightarrow$  absence of global self-similarity

Pierluigi Veltmi  
Dipartimento di Fisica, Università della Calabria

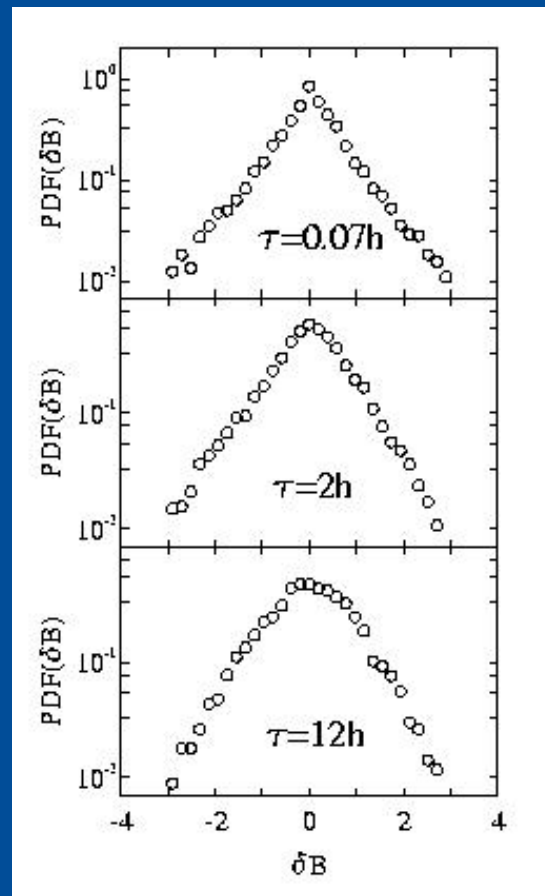
Small scales



Inertial range



Large scales



PDFs of normalized fluctuations are not Gaussians

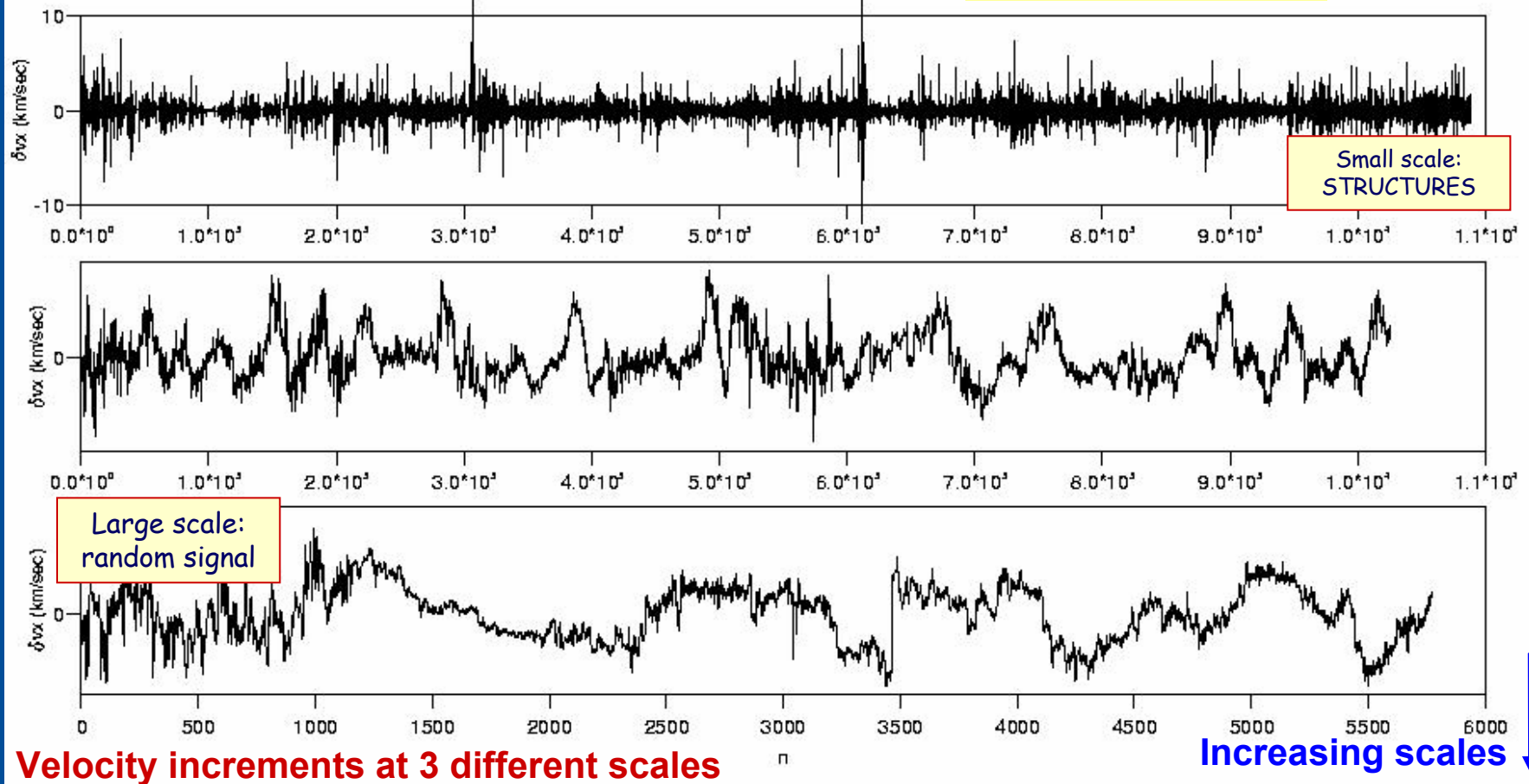
PDFs changes with scale

**Note:** The role actually played by the energy spectrum  $E(k)$  is limited in real turbulence, the phenomenon **CANNOT** be described taking into account only the 2-th order moment

# What is "intermittent" ?



## Solar Wind data



Intermittency is due to strong fluctuations confined to small scales. Scaling law depends on position: (MULTIFRACTAL)

# Wavelet analysis of **intermittent** "structures"



Intermittent "**coherent**" events within turbulence, on all scales, can be identified through **wavelet analysis**.

Wavelet transform

$$W(b, a) = C_g^{-1/2} \frac{1}{\sqrt{a}} \int_{-\infty}^{\infty} \psi\left(\frac{x-b}{a}\right) f(x) dx$$

Haar basis

$$\psi(x) = \begin{cases} 1 & 0 < x < 1/2 \\ -1 & \text{for } 1/2 < x < 1 \\ 0 & \text{elsewhere} \end{cases}$$

$a = 2^m$  scale dilation       $b = 2^m i$  position traslation

Signature of intermittency: **large isolated values of**  $|W^m(i)|^2$

Wavelet coefficient classification:

Passive

$$|W^m(i)|^2 \leq F \langle |W^m(i)|^2 \rangle$$

Intermittent

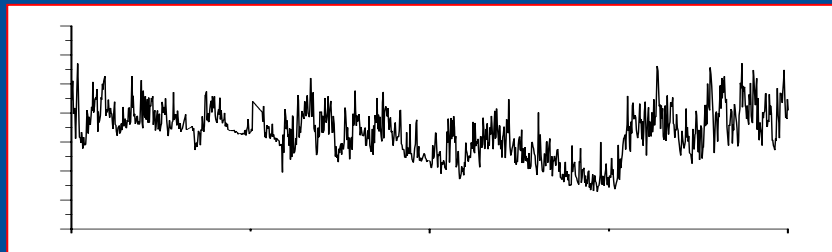
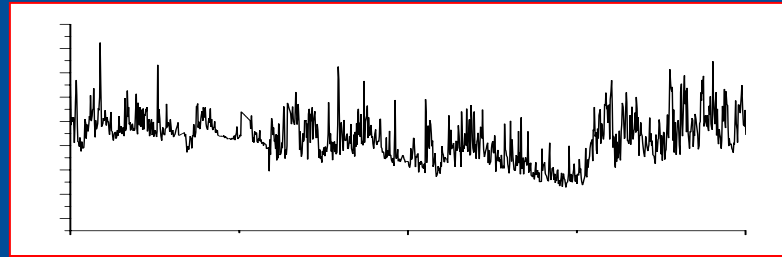
$$|W^m(i)|^2 > F \langle |W^m(i)|^2 \rangle$$

# Intermittent "structures" and background

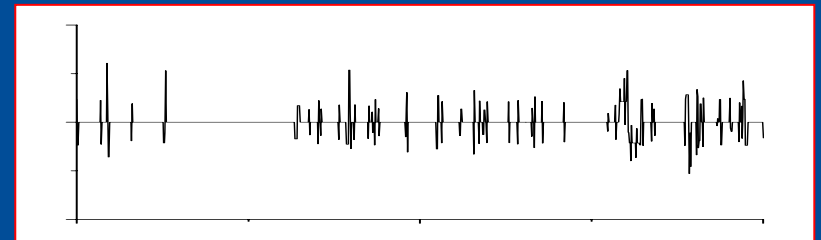


Wavelet coefficients classification ( $F = 5$ ) allows to split the time signal

Complete signal



Gaussian background



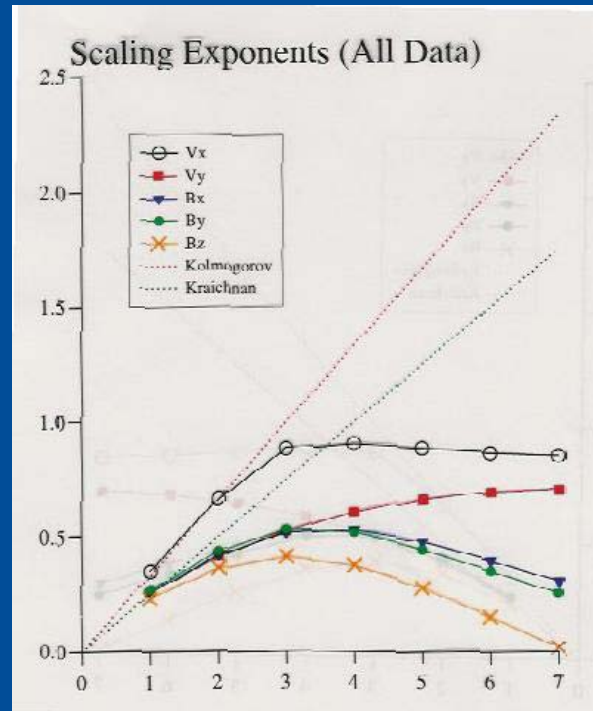
Isolated Structures



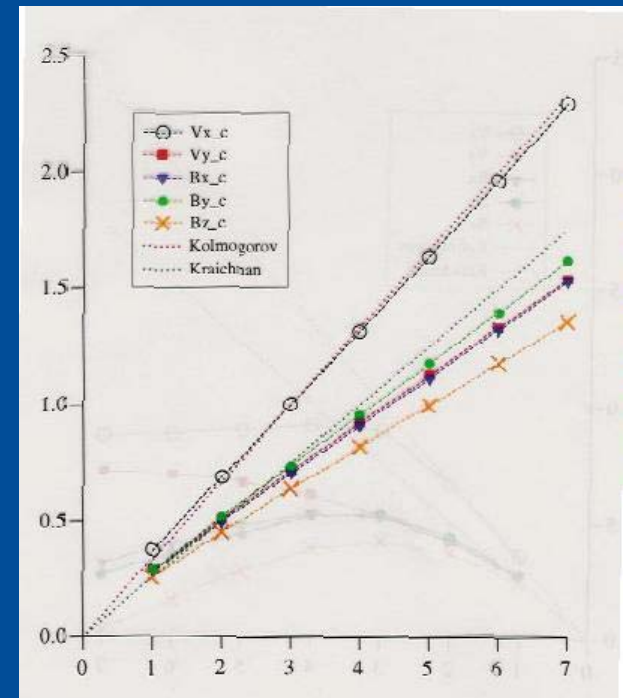
# Fractal vs multifractal behavior



After elimination of the **intermittent isolated structure** from the signal **Scaling exponents** are linear functions of the order of moment



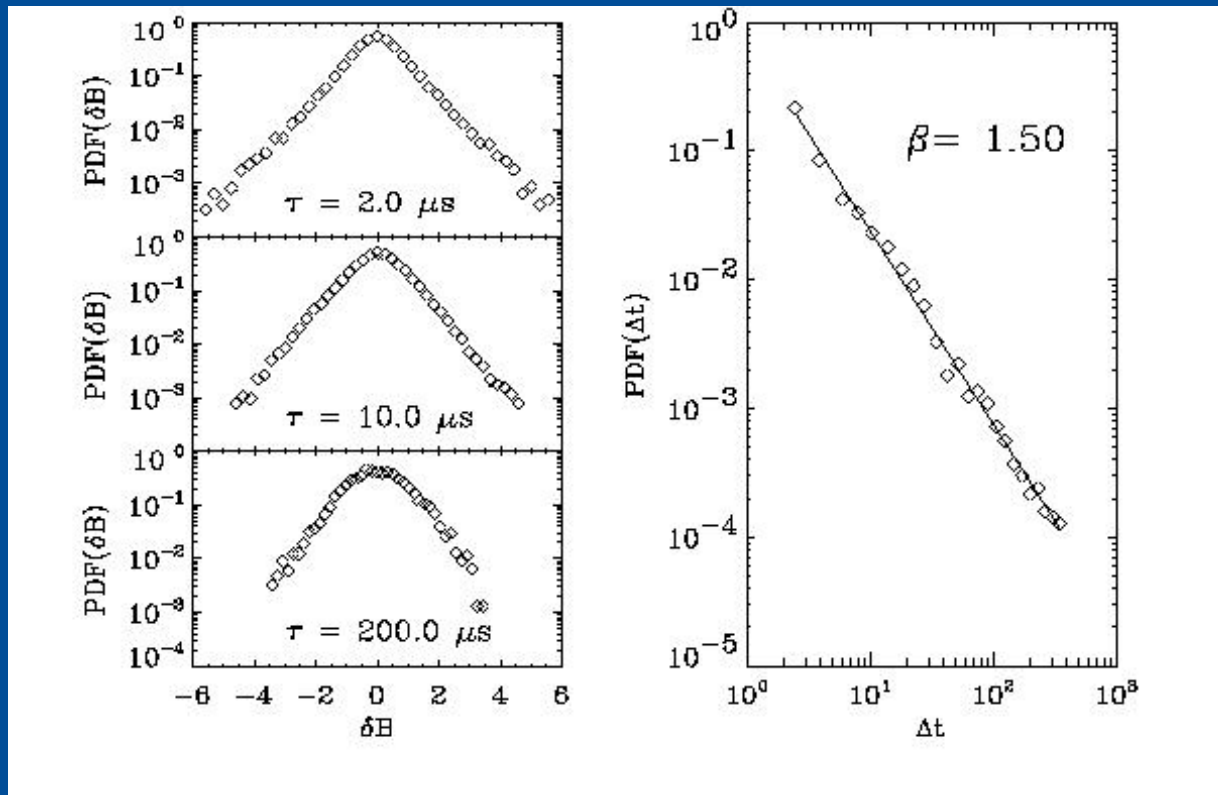
The time signal displays a **fractal (selfsimilar)** behavior



# Waiting times between structures



## Laboratory plasma




The times between events are distributed according to a power law  $\text{PDF}(\Delta t) \sim \Delta t^{-\beta}$ . The turbulent energy cascade generates intermittent "coherent" events.

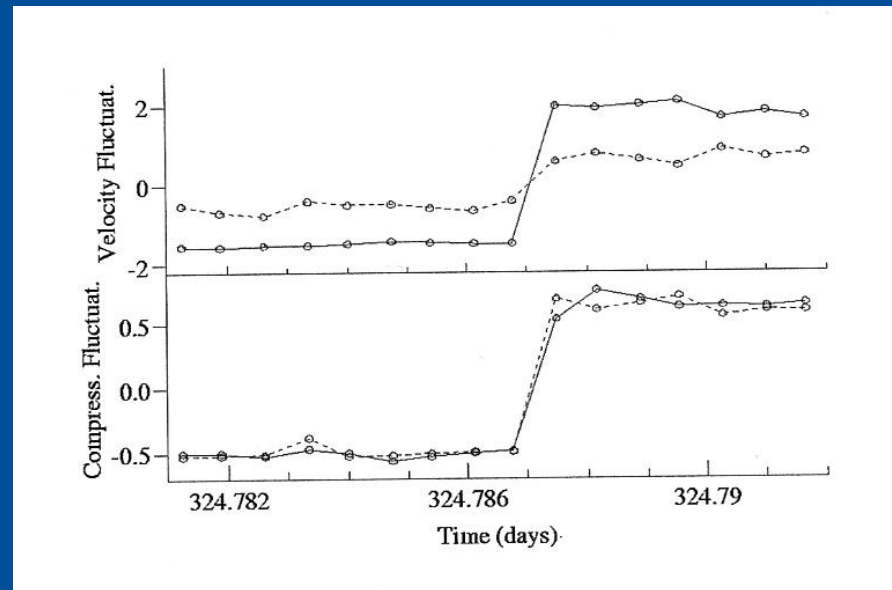
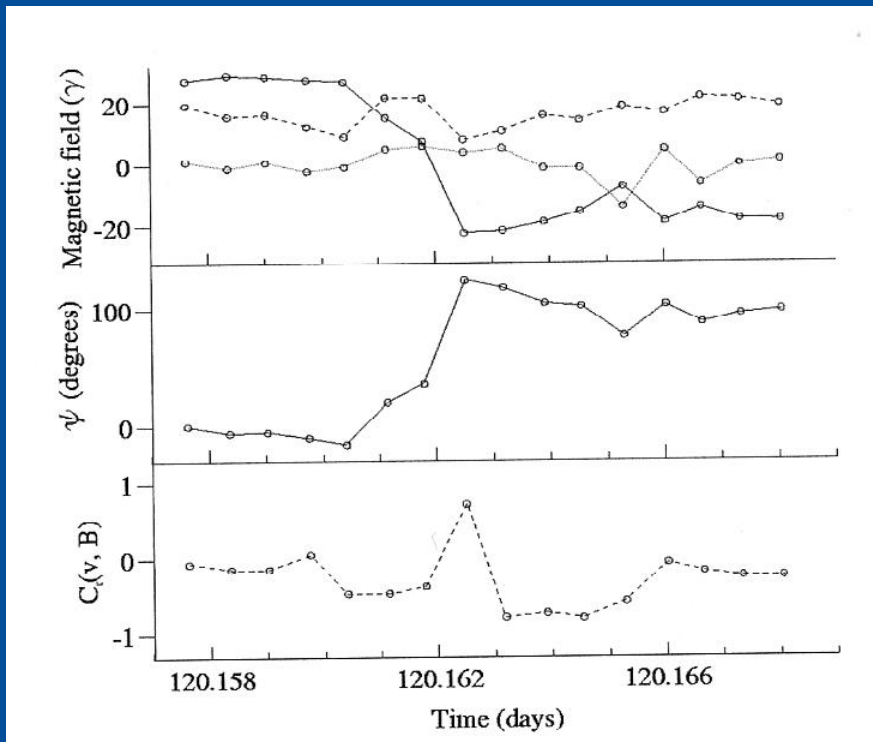
The underlying cascade process is NOT POISSONIAN, this means that the intermittent (more energetic) bursts are NOT INDEPENDENT (memory)

# What kind of **intermittent structures** ?



Minimum variance analysis around isolated structure allows to identify them

Solar Wind: **shock**   
(compressive structures)



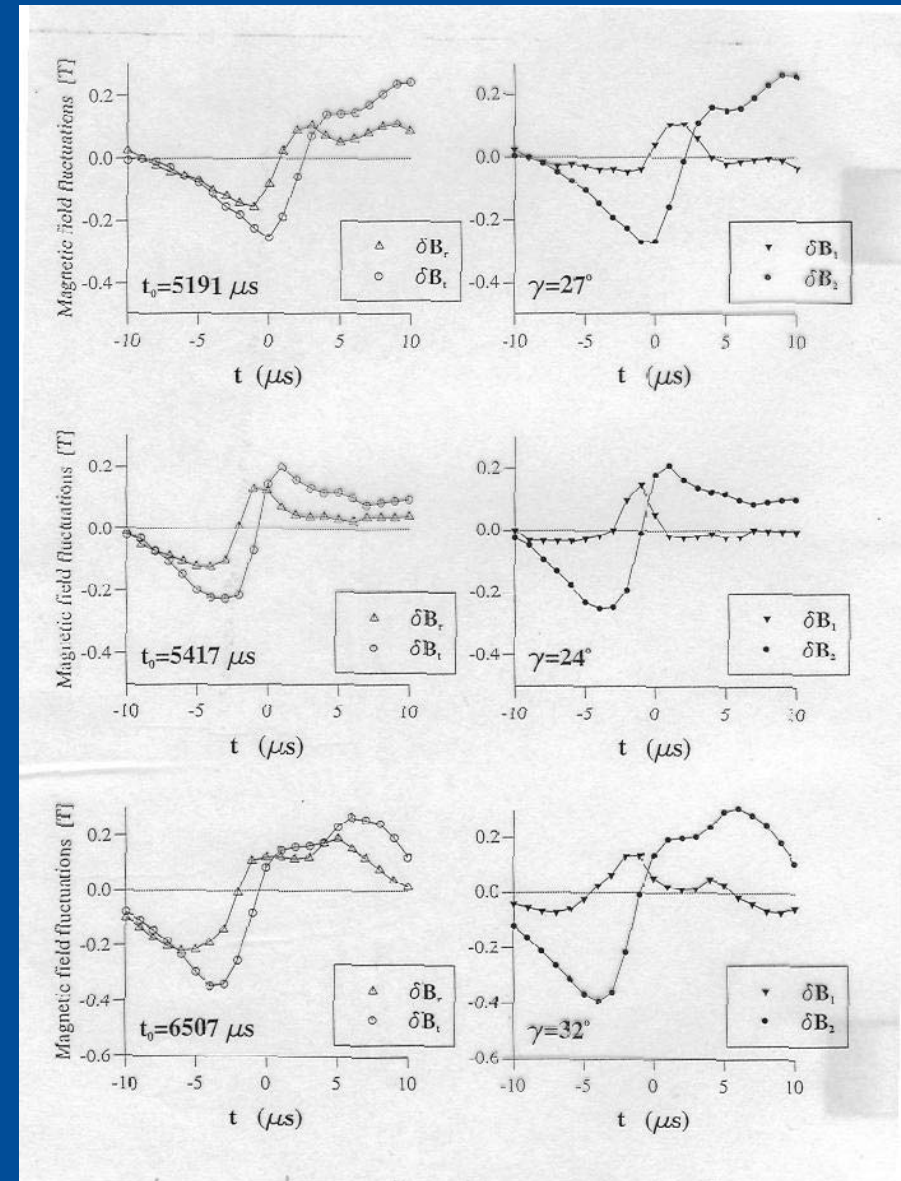
Solar wind: **tangential discontinuity (current sheet)**

# Intermittent structures in laboratory plasmas



RFX edge turbulence:  
current sheets

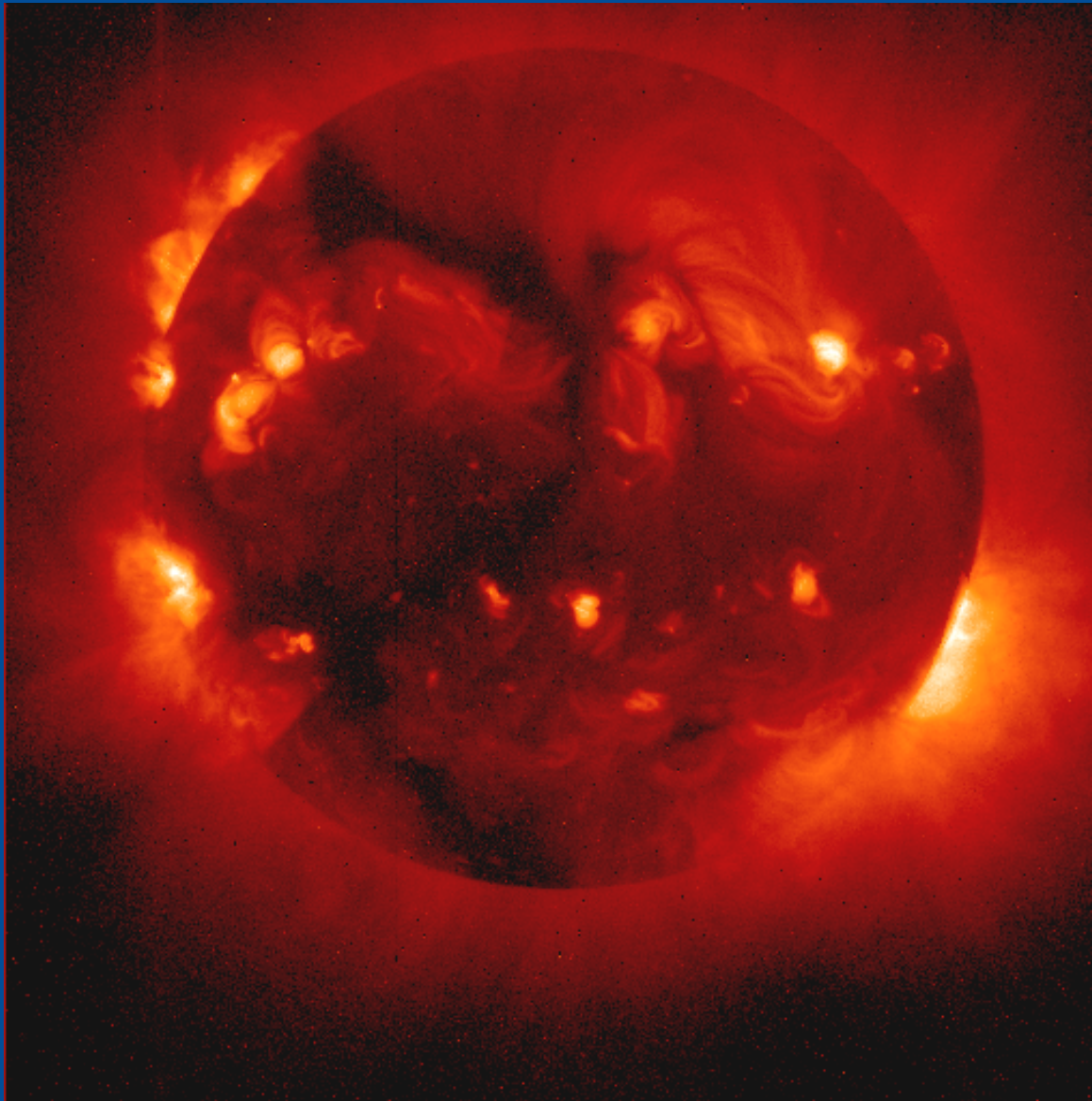
Current sheets are naturally produced as coherent, intermittent structures by nonlinear interactions



# A Statistical approach to Solar Flares



Pierluigi Veltri  
Dipartimento di Fisica, Università della Calabria



Ratio of EIT full Sun images in Fe XII 195A to Fe IX/X 171A.

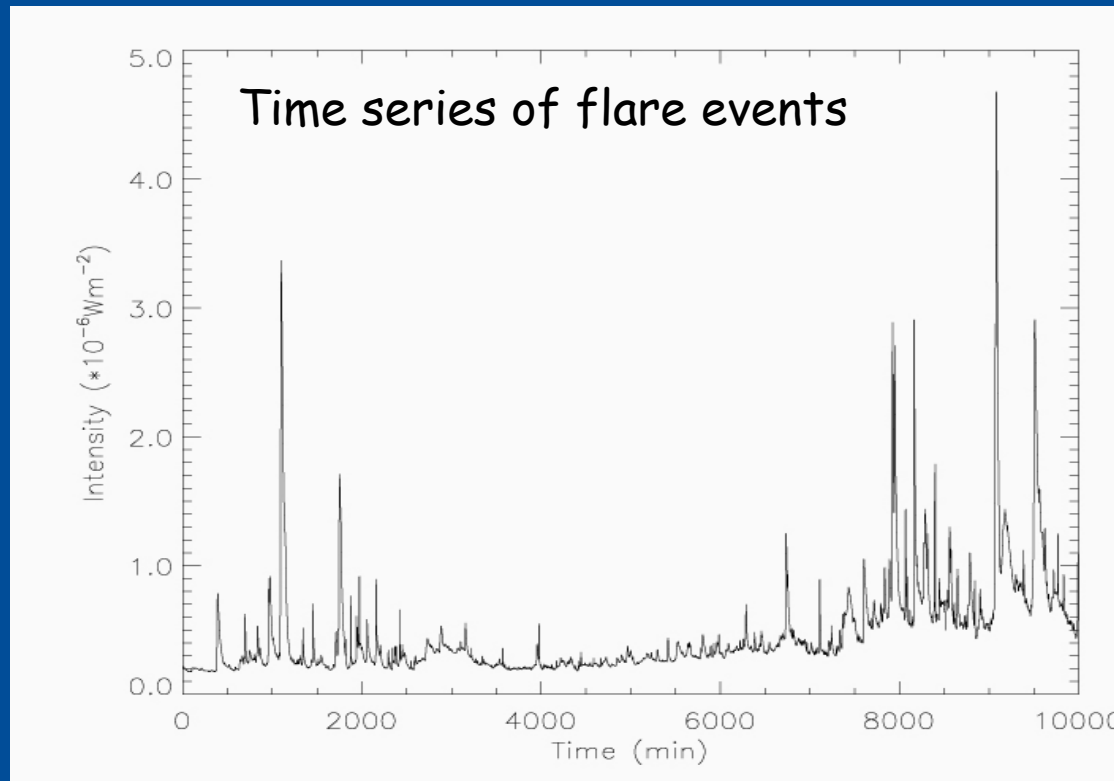
Temperature distribution in the Sun's corona:

- dark areas cooler regions
- bright areas hotter regions

# Solar flares are impulsive events



Pierluigi Veltri  
Dipartimento di Fisica, Università della Calabria



Hard X-ray ( $> 20$  keV):

Intermittent spikes

Duration 1-2 s,

$E_{\text{max}} \sim 10^{27}$  erg

Numerous smaller spikes down to  $10^{24}$  erg (detection limit)

X-ray corona: superposition of a very large number of flares

Nano flares

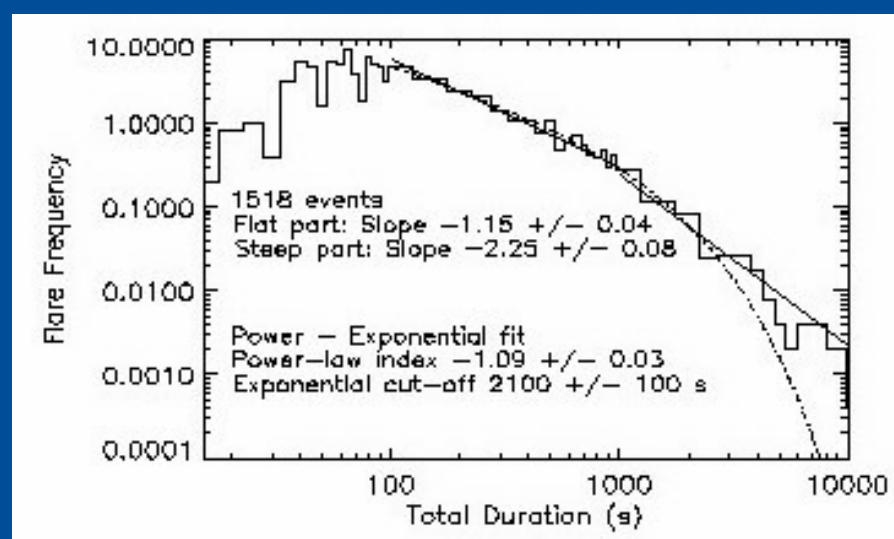
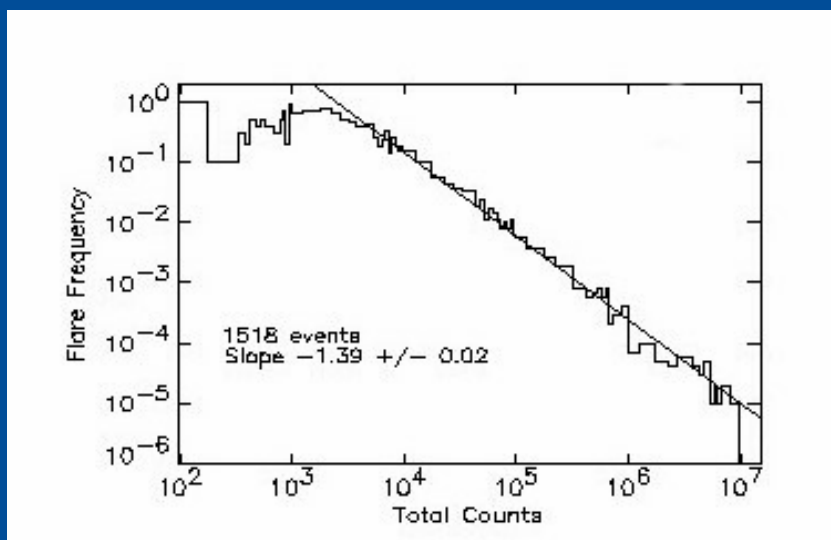
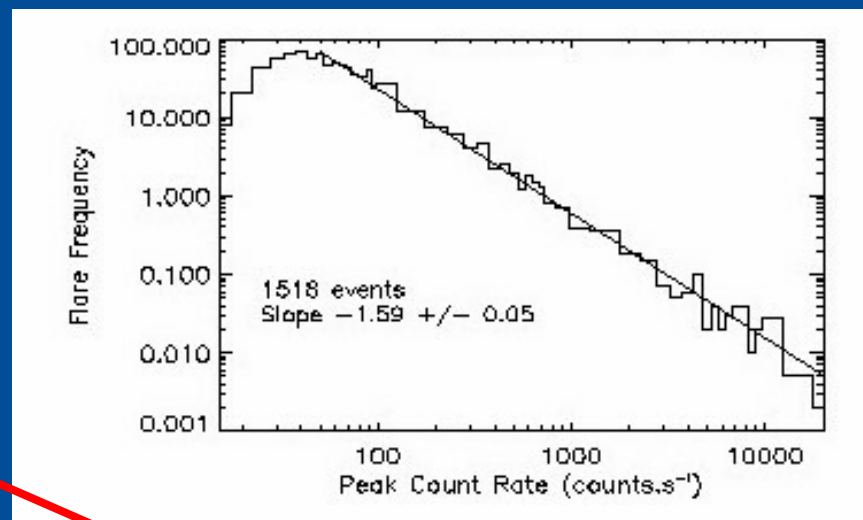
# Power laws for statistics of events



Power peak distribution

Duration distribution

Total energy distribution



# Parker's conjecture (1988)



**Nanoflares** correspond to dissipation of many small **current sheets**, forming in the **bipolar regions** as a consequence of the continuous shuffling and intermixing of the footpoints of the field in the photospheric convection.

**Current sheets:** tangential discontinuity which become increasingly severe with the continuing winding and interweaving eventually producing intense magnetic dissipation in association with magnetic reconnection,



# Self-Organized Criticality (P. Bak et al., 1987)



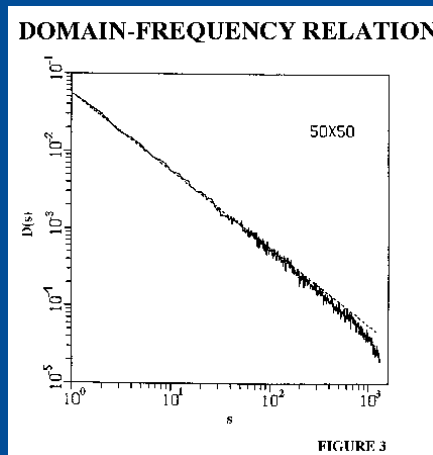
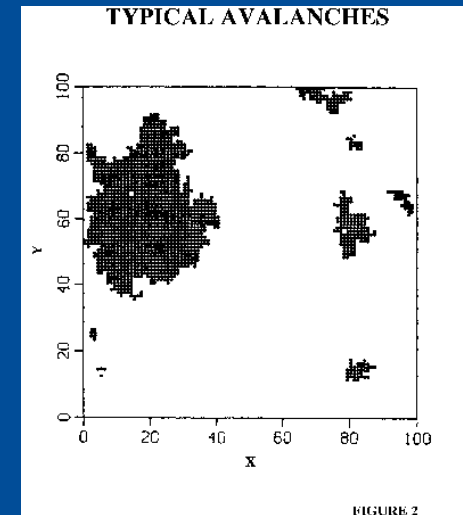
**Sand Pile** model for **Solar Flares**:

Fall of grains give rise to an avalanche whose dimension is that of the marginally stable region

Lack of any typical length



Avalanches of all size i.e. **FRACTAL PROCESS**



**Size, lifetimes and number of sand grains** in each avalanche are **power law** distributed.

# Sand Pile Model for Solar Flares (Lu & Hamilton., 1991)



Cellular Automata model for reconnection :

- Vector field  $B_i$  on a 3D lattice
- Local slope 
$$dB_i = B_i - \sum_j w_j B_{i+j}$$

When  $|dB_i| >$  some treshold: instability at position  $i$  :

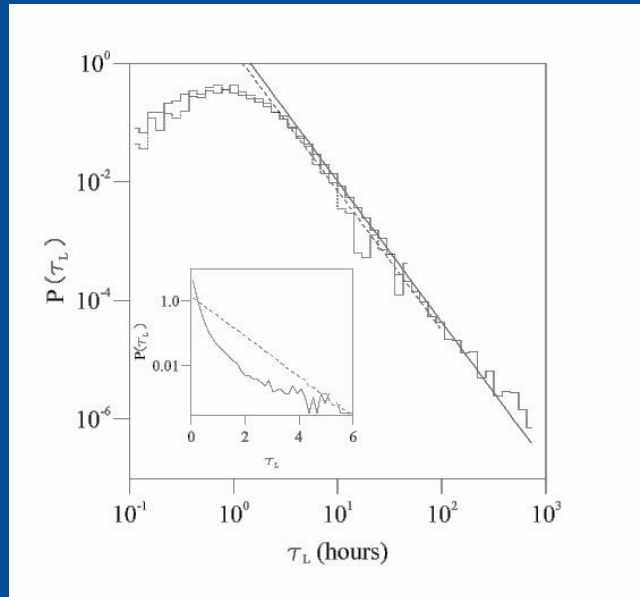
- Field readjusted in the nearby positions so that the grid point  $i$  becomes stable
- The readjustment can destabilize nearby points producing an avalanche

Power peak, total energy and duration are power law distributed.

# Waiting time distribution



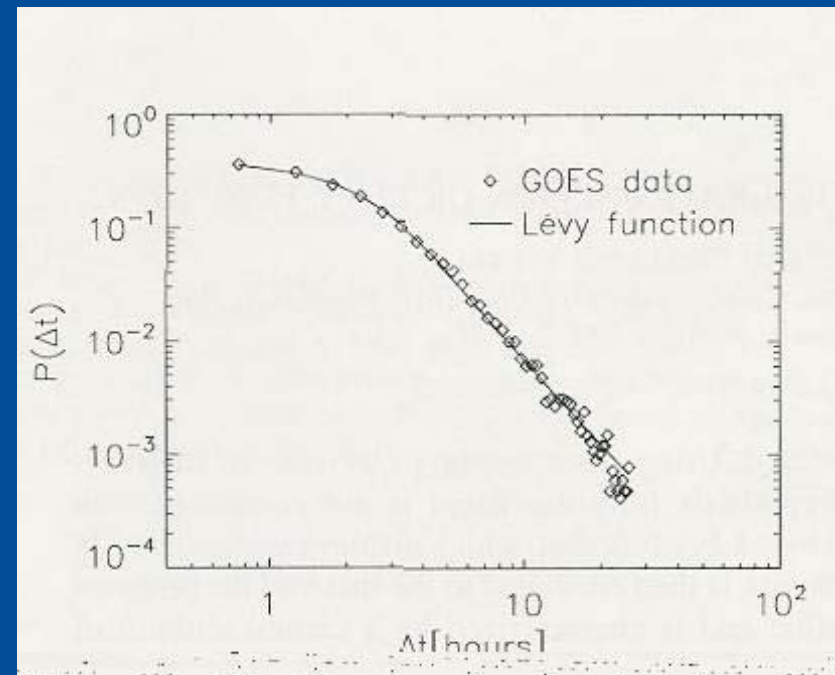
Pierluigi Veltri  
Dipartimento di Fisica, Università della Calabria



Waiting time distribution of soft X-ray nanoflares displays a power law (Boffetta et al., 1999)

SOC models naturally give rise to an exponential distribution

Waiting time distribution of soft X-ray nanoflares can be fitted with a Levy function (asymptotically power law) (Lepreti et al., 2001)



Trieste  
2003

# Parker's conjecture modified



Pierluigi Veltri  
Dipartimento di Fisica, Università della Calabria

**Nanoflares** correspond to dissipation of many small current sheets, forming in the **nonlinear cascade** occurring inside coronal magnetic structure as consequence of the **power input** in the form of **Alfven waves** due to **footpoint motion**.

**Current sheets**: coherent **intermittent** small scale structures of MHD turbulence

Trieste  
2003

# Turbulence modelling



Dynamical shell models:

Simulations of the cascade process through the dynamics of nonlinear couplings.

Allow us to obtain the time evolution of fluctuations, to find scaling laws and to describe the chaotic dynamics on the attractor in the phase space.

Geometrical description is neglected but nonlinear interactions are described at best

# MHD equations in the wave vectors space



For  
 $\sigma = +1, -1$

$$\frac{\partial z_{\alpha}^{\sigma}(\mathbf{k}, t)}{\partial t} = M_{\alpha\beta\gamma}(\mathbf{k}) \sum_p z_{\beta}^{\sigma}(\mathbf{p}, t) z_{\gamma}^{-\sigma}(\mathbf{k} - \mathbf{p}, t)$$

$$M_{\alpha\beta\gamma}(\mathbf{k}) = -ik_{\beta} \left( \delta_{\alpha\gamma} - \frac{k_{\alpha} k_{\gamma}}{k^2} \right)$$

$$z_{\alpha}^{\sigma} = u_{\alpha} + \sigma \frac{B_{\alpha}}{\sqrt{4\pi\rho}}$$

Infinite wave vectors involved in the sum,  
but the presence of dissipation introduces  
a maximum wave vector

$$k_{\max} \approx k_{\text{diss}} \approx k_0 R^{3/4}$$

Even in this case we have a large  
number of variables

$$N \approx (k_{\text{diss}} / k_0)^3 \approx R^{9/4}$$

# Dynamical (shell) models



1) Introduce a logarithmic spacing of the wave vectors space (shells);

$$k_n = k_0 2^n$$
$$n = 1, 2, \dots, N$$

2) Assign to each shell ONLY two dynamical variables;

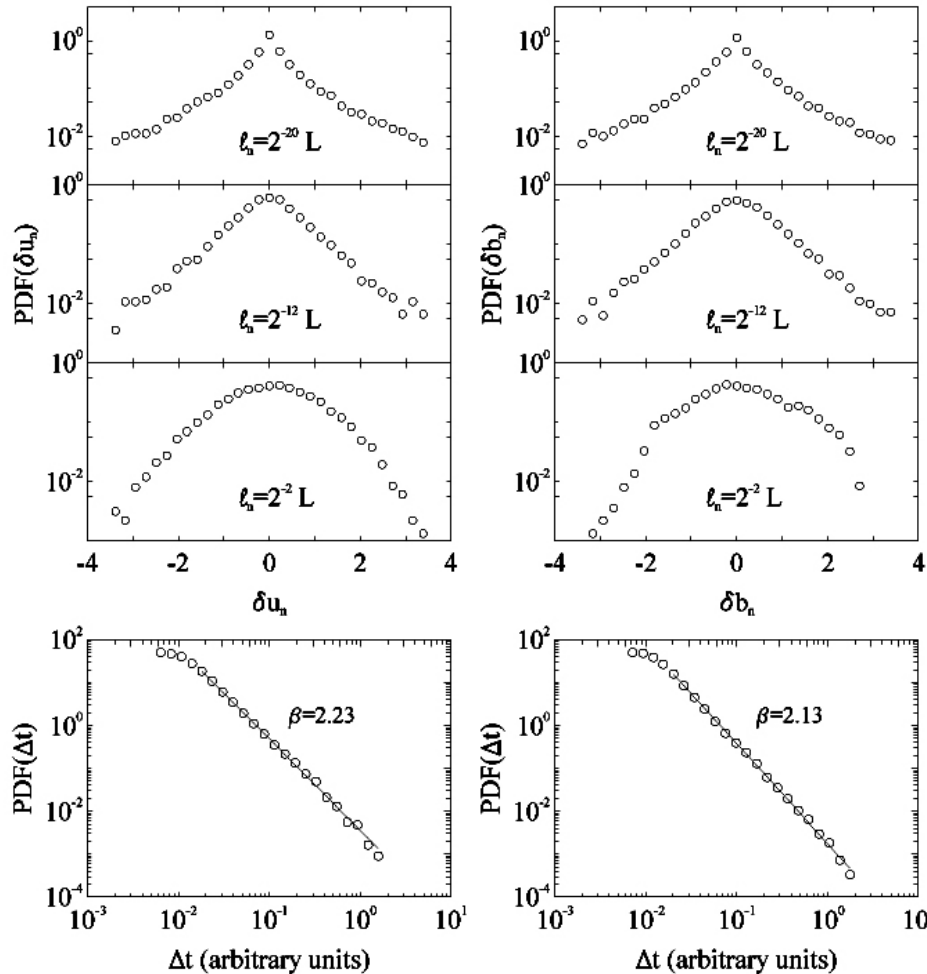
$$z_n^\pm(t) = u_n(t) \pm b_n(t)$$

3) Write a nonlinear equations with couplings among variables belonging to local shells;

$$\frac{dz_n^\pm(t)}{dt} = ik_n \sum_{i,j=\pm 2,\pm 1} M_{i,j} z_{n+i}^\pm(t) z_{n+j}^\mp(t)$$

4) Finally fix the coupling coefficients imposing the conservation of ideal invariants.

# Properties of MHD shell model



The shell model is able to capture the intermittent behaviour of real turbulence



Chaotic dynamics during the energy cascade generates non poissonian events



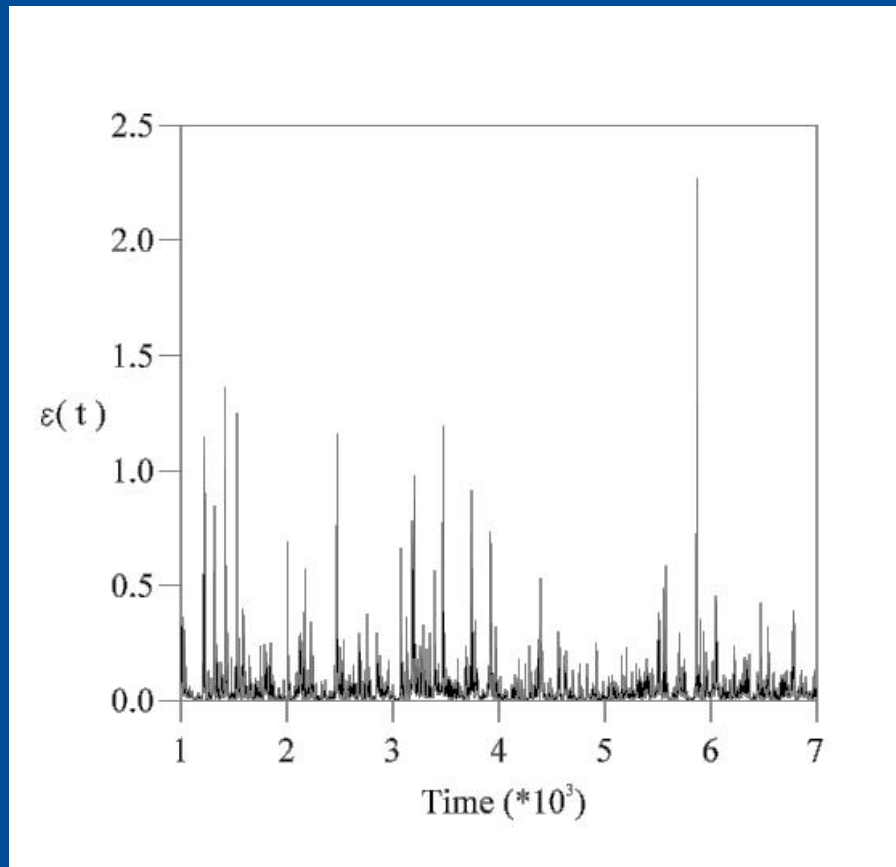
# Isolated bursts of dissipation in shell model



The energy dissipation rate is intermittent. Energy is dissipated through impulsive isolated events (bursts).

Bursts can be isolated through a threshold process to make statistics.

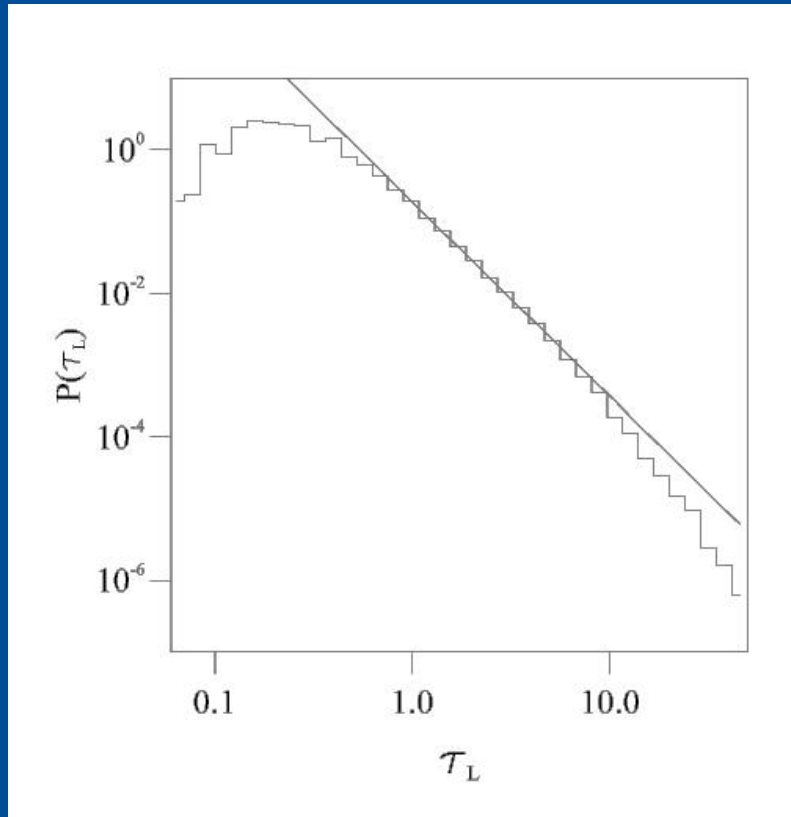
$$\varepsilon(t) = \nu \sum_n k_n^2 |u_n|^2 + \eta \sum_n k_n^2 |b_n|^2$$



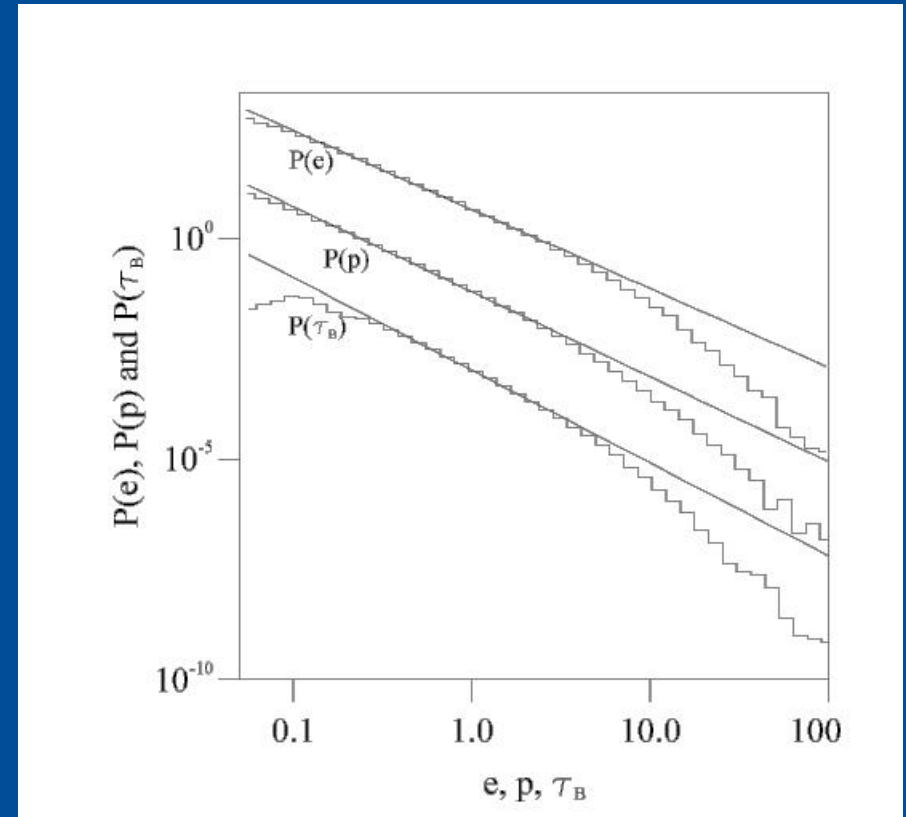
# Solar Flares: intermittent dissipative events within MHD turbulence?



Pierluigi Veltri  
Dipartimento di Fisica, Università della Calabria



The time between two bursts is  $\tau$ , we calculate the pdf  $p(\tau)$ .



- 1) Total energy of bursts
- 2) Time duration
- 3) Energy of peak

**In all cases we found power laws.**

Trieste  
2003

# MHD Turbulence in Coronal Loops



In a coronal loop:

Small beta values

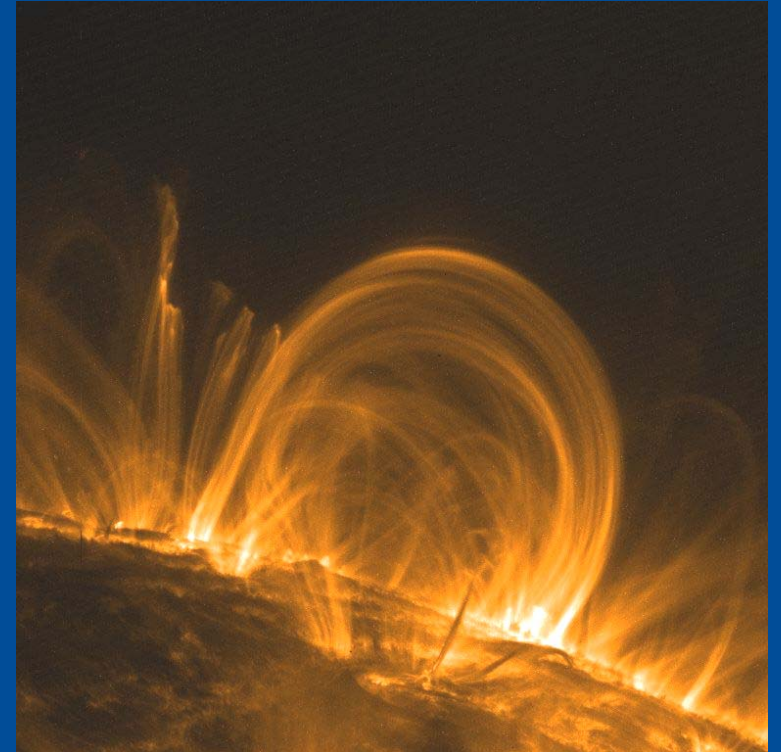
$$\beta \approx 10^{-2} \ll 1$$

Large aspect ratio

$$R = \frac{L}{L_{\perp}} \gg 1$$

Small perpendicular to parallel magnetic field ratio

$$\frac{B_{\perp}}{B_0} < \frac{1}{R} \ll 1$$



Reduced MHD can be used (RMHD):

$$\frac{\partial \mathbf{z}_{\perp}^{\sigma}}{\partial t} + \left( \mathbf{z}_{\perp}^{-\sigma} \cdot \nabla_{\perp} \right) \mathbf{z}_{\perp}^{\sigma} - \sigma c_A \frac{\partial \mathbf{z}_{\perp}^{\sigma}}{\partial x} = -\nabla_{\perp} \left( P + \frac{B^2}{8\pi} \right) + \nu \nabla_{\perp}^2 \mathbf{z}_{\perp}^{\sigma}$$

- Incompressible MHD in perpendicular variables
- Alfvén wave propagation along background magnetic field

# A Hybrid Shell Model



RMHD equations in the wave vector space perpendicular to  $\mathbf{B}_0$ :

$$\left( \frac{\partial}{\partial t} - \sigma c_A \frac{\partial}{\partial x} \right) \mathbf{z}_{\perp i}^{\sigma}(\mathbf{k}, x, t) = \sum_{\mathbf{p}} M_{ilm}(\mathbf{k}) \mathbf{z}_{\perp l}^{-\sigma}(\mathbf{p}, x, t) \mathbf{z}_{\perp m}^{\sigma}(\mathbf{k} - \mathbf{p}, x, t) - \nu k^2 \mathbf{z}_{\perp i}^{\sigma}(\mathbf{k}, x, t)$$

A **shell model** in the wave vector space perpendicular to  $\mathbf{B}_0$  can be derived:

$$\begin{aligned} \left( \frac{\partial}{\partial t} - \sigma \frac{\partial}{\partial x} \right) Z_n^{\sigma}(x, t) = & -\chi k_n^2 Z_n^{\sigma}(x, t) + \quad (3) \\ ik_n \left( \frac{11}{24} Z_{n+1}^{\sigma} Z_{n+2}^{-\sigma} + \frac{13}{24} Z_{n+1}^{-\sigma} Z_{n+2}^{\sigma} - \frac{19}{48} Z_{n+1}^{\sigma} Z_{n-1}^{-\sigma} - \right. \\ & \left. \frac{11}{48} Z_{n+1}^{-\sigma} Z_{n-1}^{\sigma} + \frac{19}{96} Z_{n-1}^{\sigma} Z_{n-2}^{-\sigma} - \frac{13}{96} Z_{n+1}^{-\sigma} Z_{n-1}^{\sigma} \right) \end{aligned}^*$$

(**Hybrid** : the space dependence along  $\mathbf{B}_0$  is kept)

# Boundary Conditions

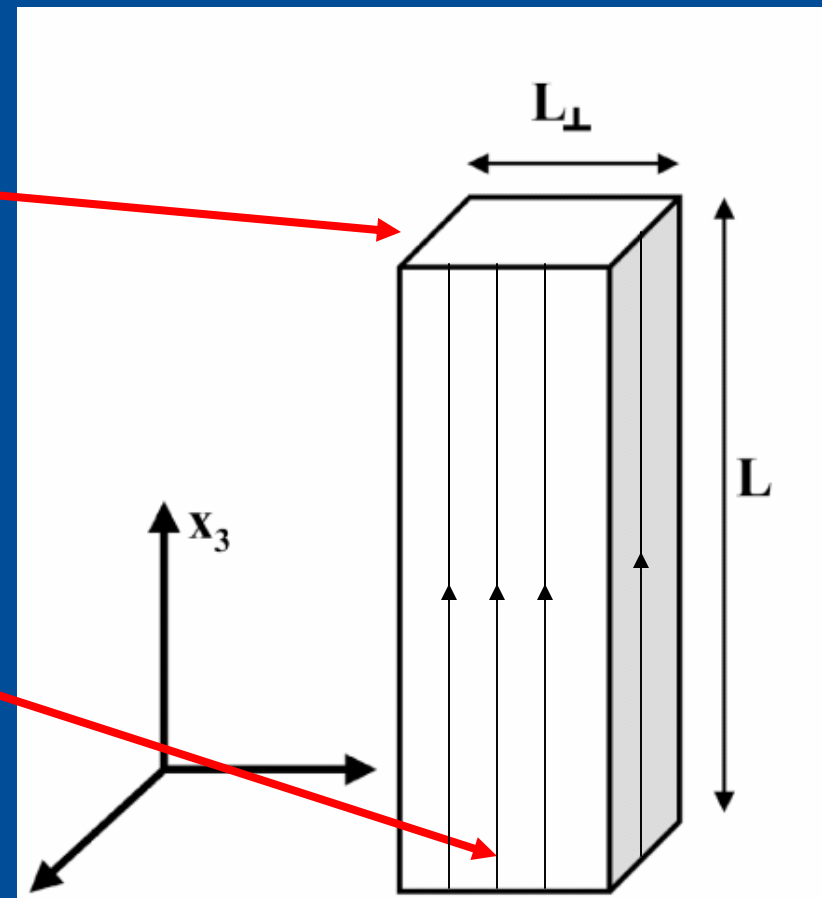


Space dependence along  $B_0$  allows to chose boundary conditions:

Total reflection is imposed at the upper boundary

A random gaussian motion with autocorrelation time  $t_c = 300$  s is imposed at the lower boundary only on the largest scales

The level of velocity fluctuations at lower boundary is of the order of photospheric motions  
 $\delta v \sim 5 \cdot 10^{-4} c_A \sim 1$  Km/s



Trieste **Model parameters:**  $L \sim 3 \cdot 10^4$  Km,  $R \sim 6$ ,  $c_A \sim 2 \cdot 10^3$  Km/s  
2003

# Energy balance

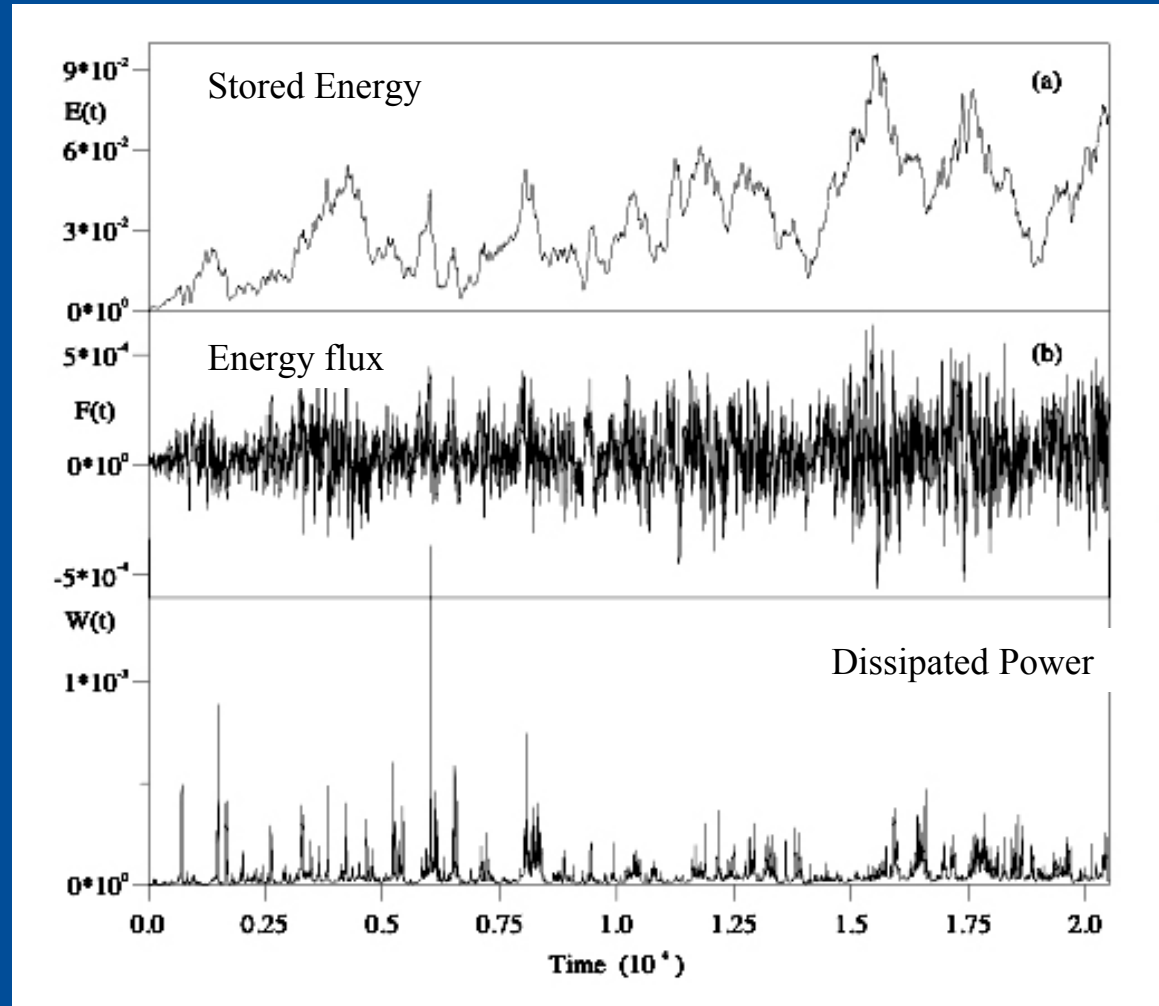


Pierluigi Veltri  
Dipartimento di Fisica, Università della Calabria

After a transient a statistical equilibrium is reached between incoming flux, outgoing flux and dissipation

The level of fluctuations inside the loop is considerably higher than that imposed at the lower loop boundary

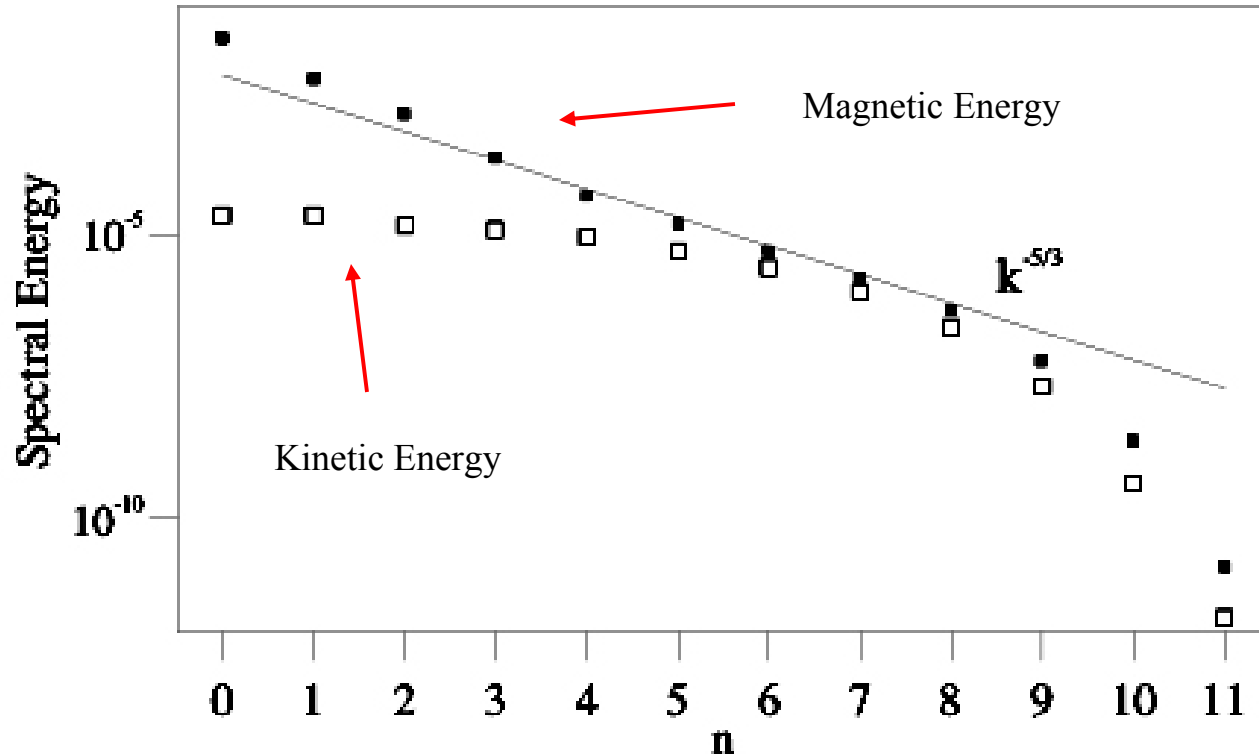
Dissipated power displays a sequence of spikes



# Energy spectra



Pierluigi Veltri  
Dipartimento di Fisica, Università della Calabria



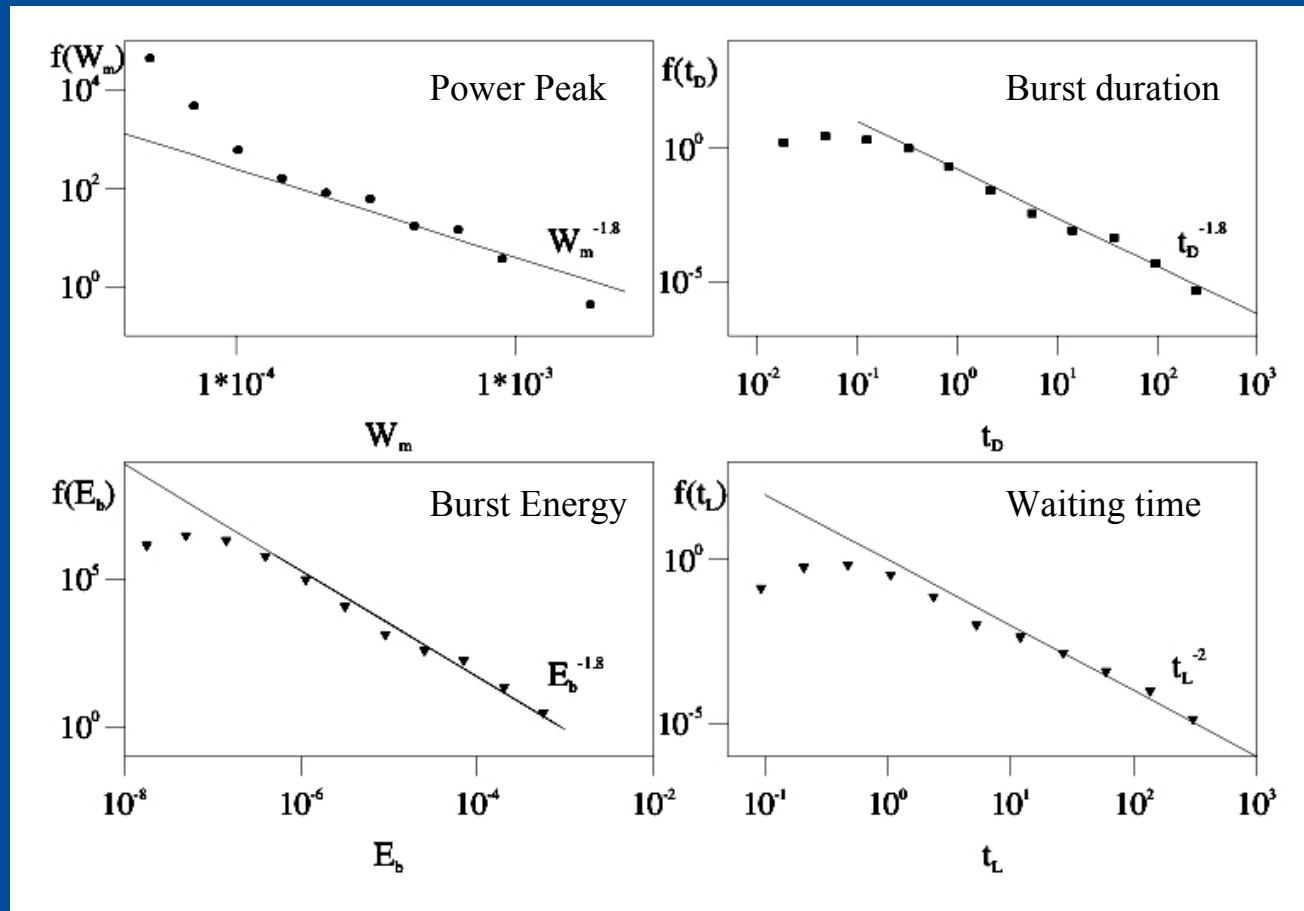
A Kolmogorov spectrum is formed mainly on magnetic energy

Magnetic energy dominates with respect to kinetic energy

# Statistical analysis of dissipated power



Pierluigi Veltri  
Dipartimento di Fisica, Università della Calabria



Power laws are recovered on Power peak, burst duration, burst energy and waiting time distributions

The obtained energy range correspond to **nanoflare** energy range



# Dissipation mechanism ?



Explicit form of dissipation terms in RMHD:

Viscous term in  $V_x$  equation

$$\eta_1 \left( \nabla_{\perp}^2 + 4 \frac{\partial^2}{\partial z^2} \right) V_x + \eta_3 \left( \nabla_{\perp}^2 + 2 \frac{\partial^2}{\partial z^2} \right) V_y$$

Viscous term in  $V_y$  equation

$$\eta_1 \left( \nabla_{\perp}^2 + 4 \frac{\partial^2}{\partial z^2} \right) V_y - \eta_3 \left( \nabla_{\perp}^2 + 2 \frac{\partial^2}{\partial z^2} \right) V_x$$

Resistive term  
in  $B_x$  equation

$$\frac{c^2}{4\pi\sigma_{\parallel}} \nabla_{\perp}^2 B_x$$

Resistive term  
in  $B_y$  equation

$$\frac{c^2}{4\pi\sigma_{\parallel}} \nabla_{\perp}^2 B_y$$

Reynolds  
Numbers

$$R_1 = \frac{VL}{\eta_1} \approx 10^{15}$$

$$R_3 = \frac{VL}{\eta_3} \approx 10^9$$

Lundquist  
Number

$$S = \frac{4\pi\sigma_{\parallel}}{c^2} Lc_A \approx 10^{14}$$

But  $\eta_3$  term does not contribute to dissipation !

Dissipation lengths much smaller than ion Larmor radius

We need an efficient Kinetic dissipation mechanism !

# Conclusions

Physical understanding of complex nonlinear phenomena occurring in plasmas require the coordinated utilization of different tools: space and laboratory data analysis, simplified dynamical models, numerical simulations.

Dynamical models, in particular, are useful to describe turbulence, intermittency, anomalous scalings of pdfs, etc.

The intermittent behavior observed in turbulent fluid flows seems to represent a key to explain some bursty phenomena occurring in space, laboratory and solar corona plasmas.

The signature of non linear interactions seems to be a multifractal behavior: SOC models being intrinsically fractal cannot adequately describe the complexity of turbulent systems. In particular they cannot naturally describe the correlations between the intermittent coherent small scale structures of turbulence.

